**Table 3 – Clinicopathological characteristics and results of immunohistochemical staining of ANXA2 and S100A10**

| Patient | Age | Gender | Hepatitis virus infection | Histological type | Vascular invasion | Annexin2 expression | S100A10 expression |
|---|---|---|---|---|---|---|---|
| Case 1 | 71 | M | HCV | por | – | ++ | ++ |
| Case 2 | 66 | F | HBV | mod | + | ++ | ++ |
| Case 3 | 38 | M | HBV | mod | + | ++ | ++ |
| Case 4 | 65 | M | HCV | por | + | ++ | ++ |
| Case 5 | 59 | M | HCV | por | – | ++ | ++ |
| Case 6 | 72 | F | HCV | mod | – | + | ++ |
| Case 7 | 71 | M | – | por | – | ++ | + |
| Case 8 | 72 | M | HBV, HCV | por | – | ++ | + |
| Case 9 | 61 | M | – | por | – | ++ | + |
| Case 10 | 78 | M | HCV | por | – | ++ | + |
| Case 11 | 49 | F | HBV | por | + | ++ | + |
| Case 12 | 72 | F | HBV | por | + | + | + |
| Case 13 | 68 | M | HBV, HCV | mod | – | + | + |
| Case 14 | 78 | F | HBV, HCV | mod | – | + | + |
| Case 15 | 74 | M | HBV, HCV | well | – | + | + |
| Case 16 | 67 | M | – | mod | – | – | + |
| Case 17 | 53 | M | HBV | mod | + | – | – |
| Case 18 | 75 | M | HCV | por | – | – | – |
| Case 19 | 66 | M | HBV, HCV | mod | + | – | – |
| Case 20 | 60 | M | HCV | por | – | – | – |

++, strong immunopositive; +, partial immunopositive; –, immunonegative.

Colocalisation of ANXA2 and S100A10 was observed in 15 samples (Table 3).

### 3.5. *Correlation between gene expression signature of the two 'hotspot' and clinicopathological features*

Next, to better understand if any of the two 'hotspot' identified by this integrated approach correlates with clinicopathological features, a hierarchical clustering of all 100 HCC samples using the upregulated genes included in the 'hotspot' was performed. Fig. 4A shows the gene expression profiles using the 11 genes upregulated in the 'hotspot 1 (integrin signalling)'. Examination of this result allowed identification of three subgroups; 'relatively high-activated group ($n = 39$), defined as Group A1', 'intermediate-activated group ($n = 45$), defined as Group A2', and 'relatively low-activated group ($n = 16$), defined as Group A3'. Likewise, Fig. 4B shows the gene expression profiles using the 12 genes upregulated in the 'hotspot 2 (Akt/NF-κB signalling)'. Examination of this result also identified two subgroups; 'relatively high-activated group ($n = 17$), defined as Group B1' and 'relatively low-activated group ($n = 83$), defined as Group B2'. Having identified the two distinctive subgroups; 'relatively high-activated group' and 'relatively low-activated group' in each of the two 'hotspots', we examined the association between the activation of 'hotspot' and clinicopathological data (Table 4A and B). In the integrin signalling, the activated profile was significantly associated with intrahepatic metastasis ($p = 0.012$), tumour size ($p = 0.023$) and Edmonson grading ($p < 0.001$). On the other hand, in the Akt/NF-κB signalling, the activated profile was significantly associated with Edmonson grading ($p = 0.004$). Kaplan–Meier plot showed a significant difference in the probability of disease-free survival ($p = 0.037$) and overall survival ($p = 0.045$) between 'Group A1' and 'Group A3' in the integrin signalling (Fig. 4C and D). In the Akt/NF-κB signalling, a significant difference was observed in disease-free survival ($p = 0.045$, Fig. 4E and F).

### 3.6. *Overview of the distribution of differentially expressed genes on human chromosome*

To compare our microarray data with chromosomal aberrations in HCC, we also investigated the chromosomal region in which the differentially expressed genes were harboured. The public source for annotating the location of each gene was the National Center for Biotechnology Information (NCBI). This investigation revealed that the regions of high density of 100 upregulated genes tended to be at chromosomes 1q, 6p and 8q (Fig. 5A), whilst those of 100 downregulated genes were at chromosomes 4q and 16q (Fig. 5B). Furthermore, SPP1, GPC3, ANXA2 and S100A10, identified as key molecules, were separately located at chromosomes 4q, Xq, 15q and 1q.

## 4. Discussion

In the post-genomic period, DNA microarray technology is used to monitor disease progress and to individualise treatment regimens. However, extracting new biological insights from high-throughput genomic studies of cancer progression poses a challenge due to difficulties in recognising and evaluating relevant biological processes from vast quantities of experimental data. Although other high-throughput technologies in protein expression (proteomics) and low-molecular weight metabolite expression (metabolomics) have made remarkable progress, no comprehensive analytical techniques exist that can measure more than 500,000 protein forms and 100,000–1,000,000 metabolites quantitatively.[16] Generating biological networks from comprehensive gene expression profiles manually in a visual manner could be used to navigate

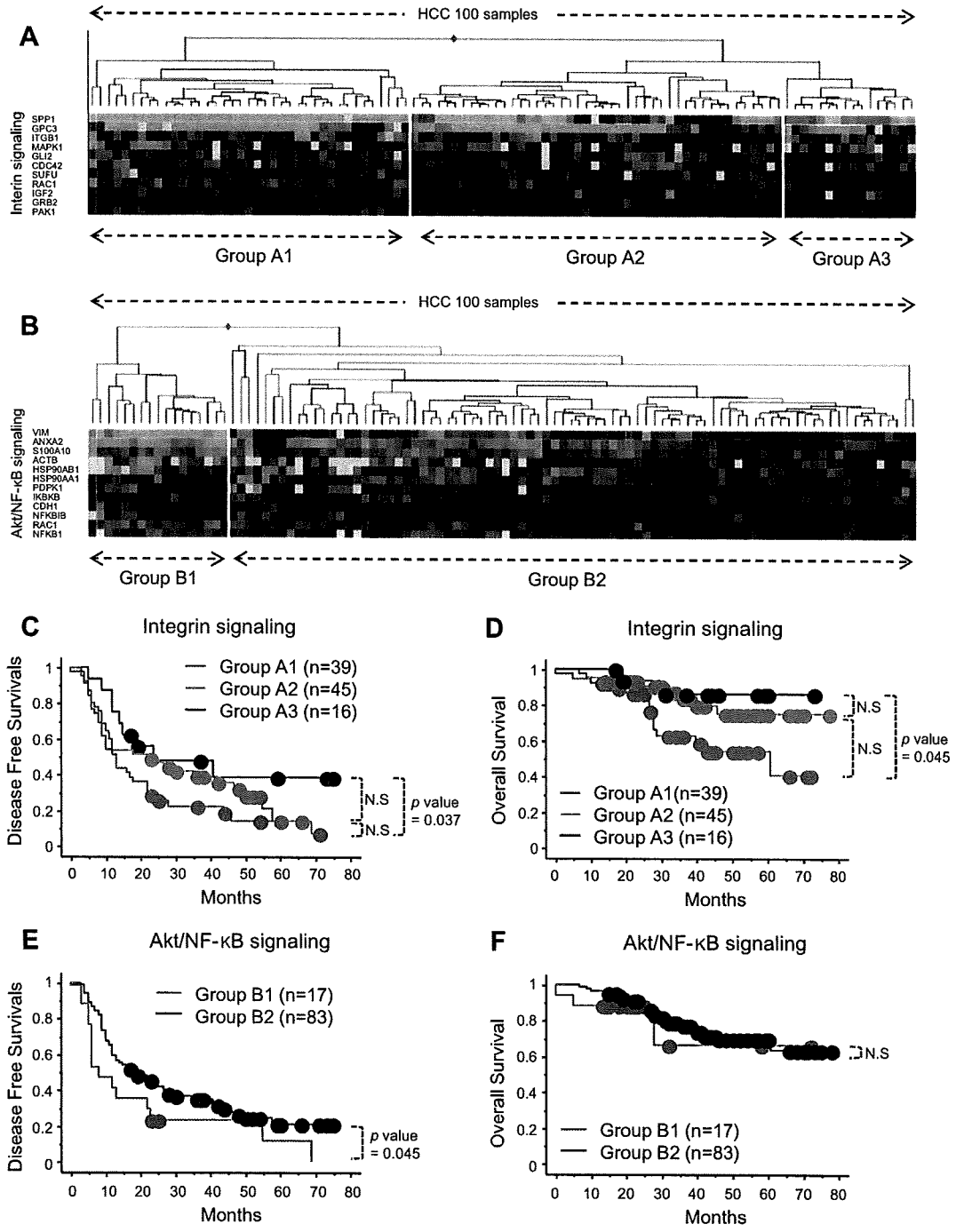


**Fig. 4 – (A) Hierarchical clustering analysis of all 100 HCC samples using the 11 upregulated genes included in the 'hotspot 1 (integrin signalling)'. Red and green indicate relative high- and low-expression, respectively. Based on the similarities of their gene expression profiles, samples were grouped in 'relatively high-activated group ($n$ = 39), defined as Group A1', 'intermediate-activated group ($n$ = 45), defined as Group A2', and 'relatively low-activated group ($n$ = 16), defined as Group A3'. (B) A hierarchical clustering analysis of all 100 HCC samples using the 12 upregulated genes included in the 'hotspot 2 (Akt/NF-κB signalling)'. Based on the similarities of their gene expression profiles, samples were grouped in 'relatively high-activated group ($n$ = 17), defined as Group B1' and 'relatively low-activated group ($n$ = 83), defined as Group B2'. (C and D) Disease-free survival and overall survival of each of the activated groups in the 'hotspot 1 (integrin signalling)' (Kaplan–Meier plot). The log-rank $p$ value is shown. NS, not significant. (E and F) Disease-free survival and overall survival of each of the activated groups in the 'hotspot 2 (Akt/NF-κB signalling)' (Kaplan–Meier plot). The log-rank $p$ value is shown. NS, not significant.**

**Table 4 – Clinical and pathological characteristics of the high-activated and low-activated groups in each of integrin signalling and AKT/NF-κB signalling**

| Characteristics | Integrin signalling ('Hotspot' 1) | | | *p* value |
|---|---|---|---|---|
| | Group A1 ($n = 39$) | Group A2 ($n = 45$) | Group A3 ($n = 16$) | |
| | No. of patients (%) | No. of patients (%) | No. of patients(%) | |
| A | | | | |
| Intrahepatic metastasis | 12(30.8) | (10(22.2)) | 0(0) | 0.012 |
| Tumour size (cm) | 4.79 ± 3.12 | (3.49 ± 1.75) | 2.91 ± 1.22 | 0.023 |
| Edmonson grading | | | | |
| 1–2 | 11(28.2) | 22(48.9) | 10(62.5) | <0.001 |
| 3–4 | 28(71.8) | 23(51.1) | 6(37.5) | |
| Pathological stage | | | | |
| I | 5(12.8) | 15(33.3) | 3(18.7) | 0.642 |
| II | 22(56.4) | 20(44.4) | 10(62.5) | |
| III | 9(23.1) | 8(17.8) | 3(18.7) | |
| IVA | 3(7.7) | 2(4.5) | 0 | |

| Characteristics | Akt/NF-κB signalling ('Hotspot' 2) | | *p* value |
|---|---|---|---|
| | Group B1 ($n = 17$) | Group B2 ($n = 83$) | |
| | No. of patients (%) | No. of patients (%) | |
| B | | | |
| Intrahepatic metastasis | 4(23.5) | 18(21.7) | 0.867 |
| Tumour size (cm) | 4.55 ± 2.58 | 3.88 ± 2.81 | 0.226 |
| Edmonson grading | | | |
| 1–2 | 2(11.7) | 41(49.4) | 0.004 |
| 3–4 | 15(88.3) | 42(50.6) | |
| Pathological stage | | | |
| I | 1(5.9) | 22(26.5) | 0.333 |
| II | 11(64.7) | 41(49.4) | |
| III | 4(23.5) | 16(19.3) | |
| IVA | 1(5.9) | 4(4.8) | |

*p* values of A are obtained by comparing Group A1 with Group A3.
*p* values of B are obtained by comparing Group B1 with Group B2.
*p* values for intrahepatic metastasis, Edmonson grading and pathological stage are obtained by $\chi^2$ test.
*p* value for tumour size is obtained by t test.
Tumour size is mean ± SD.

through and unravel the complex networks involved in cancer progression. Here, we combined genome-wide expression analysis with a new bioinformatics method, Ingenuity Pathway Analysis, to clarify the relationship between the microarray datasets and the canonical pathways based on the published literature and identify functional networks, 'hotspot', responsible for the progression of HCC. Furthermore, we discovered several molecules commonly upregulated in HCC as potential key players in the neoplastic process.

This combined approach revealed that several distinct regions with upregulated genes were concentrated. These concentrations of activated genes included several genes involved in the WNT signalling pathway, which has been the subject of intense research in recent years. In addition, we highlighted integrin and Akt/NF-κB as two 'hotspot' signalling pathways, and propose that these signalling pathways are crucial for the core biological functions in HCC progression and potential intervention, such as cell proliferation, cell survival and apoptosis.[17]

In addition to studies of gene expression at the transcriptional level, protein analysis is vital for understanding the regulatory processes in living organisms, because emerging evidence suggests that mRNA expression patterns themselves are necessary but insufficient for quantitative description of biological systems. So far, comparative studies of mRNA and protein abundance indicate that only 20–28% of the total variation of protein abundance can be attributed to mRNA abundance alone.[18] The limiting factors were explained partly by translational processes (microRNAs repress the translation of mRNAs into proteins) and post-translational modification (such as phosphorylation, methylation, acetylation, glycosylation and ubiquitination). In fact, this was the basis for investigating the expression levels of proteins encoded by highly upregulated genes related to key signalling pathways in hepatocarcinogenesis.

Using our analysis protocol, integrin pathway-associated molecules, SPP1 and GPC3, were first identified as key for cell proliferation in HCC. HCC generally spreads throughout the

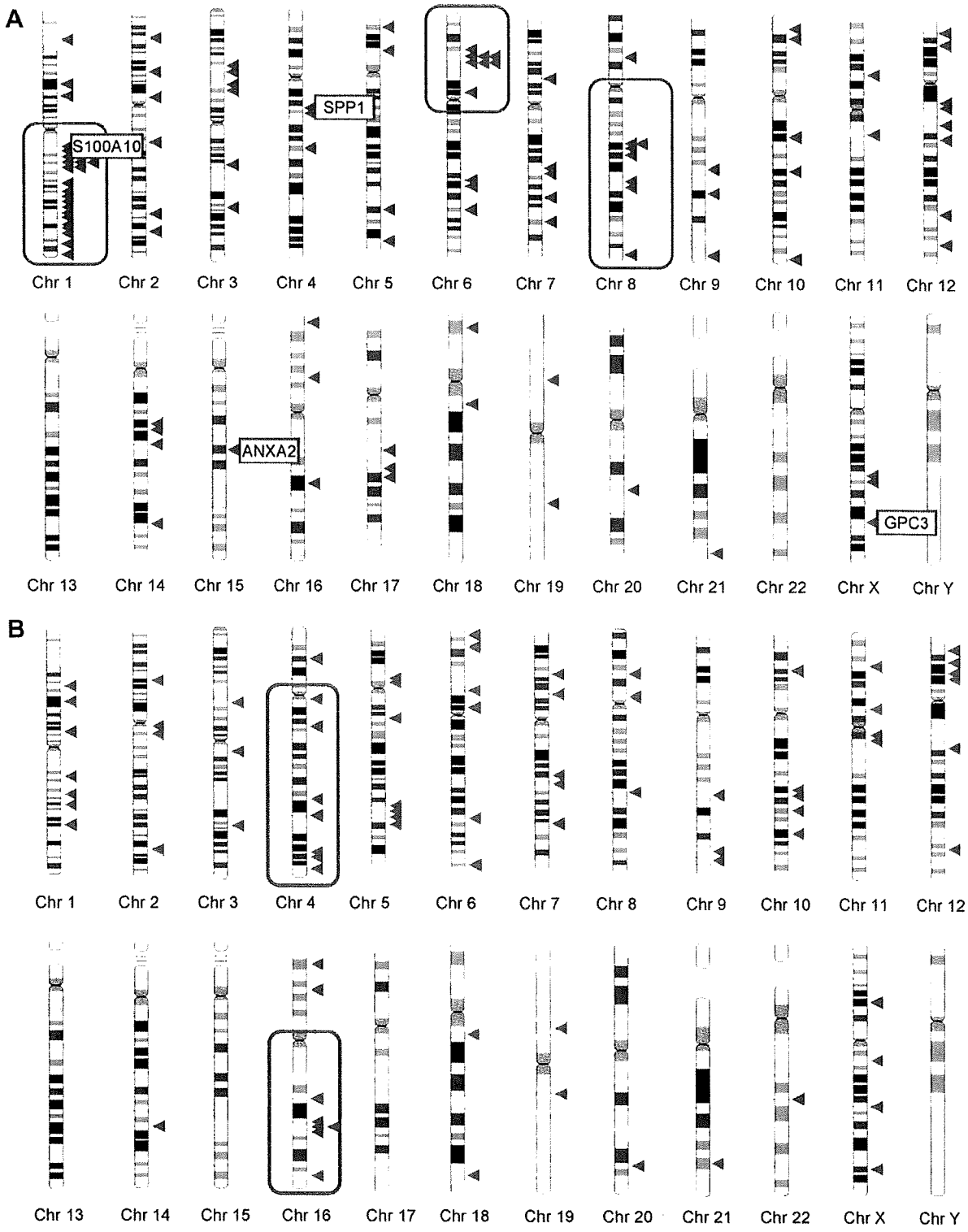


**Fig. 5 – Location of 100 upregulated genes (A) and 100 downregulated genes (B) on human chromosomes. Upregulated genes are represented as red arrows, and downregulated genes are represented as blue arrows. Red-coloured circles (chromosomes 1q, 6p and 8q) represent regions with relative concentration of upregulated genes, whilst blue coloured circles (chromosomes 4q and 16q) represent regions with relative concentration of down-regulated genes. ANXA2, S100A10, SPP1 and GPC3 are located at chromosomes 15q21-22, 1q22, 4q21-25 and Xq26.1, respectively.**

liver via the portal vein system even in advanced stages, and portal vein invasion is the most crucial histological feature associated with poor prognosis.[3] SPP1 protein expression is upregulated in primary HCC with accompanying metastasis, and SPP1 expression correlates with the invasiveness of HCC cells in tissue culture.[19] Based on network analysis, we speculated that the binding of integrins to SPP1[20] might be related to the progression and metastasis of HCC. GPC3, a heparan sulphate proteoglycan anchored to the plasma membrane, is also a good candidate marker of HCC. It is an oncofoetal protein overexpressed in HCC at both the mRNA and protein levels.[11] We also confirmed that GPC3 was overexpressed in HCC by the immunostaining of paraffin sections. In the activated integrin pathway, GPC3 interacts with IGF-2,[21] a protein that increases the phosphorylation of MAPK1.[22] GPC3 is also related to the zinc-finger transcription factors, GLI1 and GLI2, that are known players in WNT signalling and Sonic hedgehog signalling pathways.[23] Recently, WNT signalling was implicated in hepatocyte proliferation, which could be crucial in liver development, regeneration following partial hepatectomy, and pathogenesis of HCC.[24] In this context, SPP1 and GPC3 might participate in the activation of integrin signalling in HCC and based on the results of clustering analysis, might be implicated as mediators of intrahepatic metastasis, histopathological malignancy or poor prognosis.

Second, we focused on ANXA2, S100A10 and VIM, which were related to the Akt/NF-κB signalling pathway. ANXA2, also called calpactin I heavy chain, is a member of the annexin family of $Ca^{2+}$- and phospholipid-binding proteins and forms a heterotetrameric complex with S100A10, also called calpactin I light chain.[25] The ANXA2-S100A10 complex has been implicated in the structural organisation and dynamics of endosomal membranes, the organisation of cholesterol-rich membrane microdomains, and connecting lipid rafts with the actin cytoskeleton.[25] The ANXA2-S100A10 complex was also recently associated with recycling endosomes, and might be involved in the recycling of E-cadherin during the formation of the E-cadherin-based adherens junctions via the modulation of the actin cytoskeleton.[26] Moreover, ANXA2 was identified as a Rac binding partner and Rac activation is induced by the interactions of E-cadherin in the formation of adherens junctions.[27] In this way, cadherin–cadherin interactions initiate a cascade of signalling events that result in increased cadherin/Akt association, activation of Akt/NF-κB signalling, and increased cell survival and tumour growth.[27] Akt1 was found to associate structurally with VIM (a structural component of intermediate filaments),[28] which has been found in poorly differentiated HCC as well as hepatoblastomas.[29] Therefore, it is possible that binding of Akt1 and VIM activates downstream players (NF-κB signalling) as well as increasing the intrinsic activity of Akt1. This molecular understanding of HCC progression in Akt/NF-κB signalling was not so different from our result of correlations between clinicopathological features and gene expression profiles. It seems that the higher-activated group in Akt/NF-κB signalling has lower histopathological differentiation.

Currently, the array-based CGH approach is used to study chromosomal aberrations in human cancers. A previously reported meta-analysis[30] showed that the most common chromosomal arms containing gains were 1q, 6p and 8q, whereas the most common losses were found in chromosomes 4q, 8p and 16q. Comparing our expression data with the meta-analysis result of array-based CGH in HCC,[30] we found that our gene expression data surprisingly matched the chromosomal aberrations. The comprehensive analysis of 100 HCC samples using human 30 K DNA microarray revealed a potential association between the global copy number and expression. It is also noteworthy that our identified key molecules that operate synergistically in hepatocarcinogenesis are located at separate chromosomes, so chromosomal aberrations cannot prove a relationship of candidate genes such as ANXA2 and S100A10. Therefore, our integrative network approach can provide a significant clue to the discovery of novel genetic combinations that may be important for hepatocarcinogenesis.

Here, we highlighted the 'hotspot' canonical pathways in HCC and improved our molecular understanding of HCC progression. It is widely recognised that there are distinct molecular subtypes of HCC in the transcriptome space, and current interest of the community spread to include identification of subtype-specific aberration of genes/pathway. This functional genomics study could contribute towards the detection of several signalling pathways commonly activated in HCC. Moreover, we succeeded in detecting two potential disease markers, ANXA2 and S100A10, whose colocalisation in human HCC tissues has not been reported previously.

In conclusion, we reported an integrative approach of genome-wide microarray analysis and network analysis in HCC. This novel approach allows the extraction of deeper biological insight from microarray data and identifying potential key molecules in hepatocarcinogenesis.

## Conflict of interest statement

None declared.

## Acknowledgements

We thank EIJI MIYOSHI, Department of Biochemistry, Osaka University Medical School, and JORGE FILMUS, Division of Molecular and Cell Biology, Sunnybrook and Women's College Health Sciences Centre and Department of Medical Biophysics, University of Toronto, for providing a monoclonal antibody of GPC3.

## Appendix A. Supplementary material

Supplementary data associated with this article can be found, in the online version, at doi:10.1016/j.ejca.2008.02.019.

REFERENCES

1. Thomas MB, Abbruzzese JL. Opportunities for targeted therapies in hepatocellular carcinoma. *J Clin Oncol* 2005;23:8093–108.

2. Jemal A, Murray T, Ward E, Samuels A, Tiwari RC, Ghafoor A. Cancer statistics, 2005. *CA Cancer J Clin* 2005;**55**:10–30.
3. Pan HW, Ou YH, Peng SY, Liu SH, Lai PL, Lee PH. Overexpression of osteopontin is associated with intrahepatic metastasis, early recurrence, and poorer prognosis of surgically resected hepatocellular carcinoma. *Cancer* 2003;**98**:119–27.
4. Tsou AP, Wu KM, Tsen TY, Chi CW, Chiu JH, Lui WY. Parallel hybridization analysis of multiple protein kinase genes: identification of gene expression patterns characteristic of human hepatocellular carcinoma. *Genomics* 1998;**50**:331–40.
5. Schadt EE, Monks SA, Drake TA, Lusis AJ, Che N, Colinayo V. Genetics of gene expression surveyed in maize, mouse and man. *Nature* 2003;**422**:297–302.
6. Brem RB, Yvert G, Clinton R, Kruglyak L. Genetic dissection of transcriptional regulation in budding yeast. *Science* 2002;**296**:752–5.
7. Thorgeirsson SS, Grisham JW. Molecular pathogenesis of human hepatocellular carcinoma. *Nat Genet* 2002;**31**:339–46.
8. Slaton JW, Perrotte P, Inoue K, Dinney CP, Fidler IJ. Interferon-alpha-mediated down-regulation of angiogenesis-related genes and therapy of bladder cancer are dependent on optimization of biological dose and schedule. *Clin Cancer Res* 1999;**5**:2726–34.
9. Yamamoto T, Nagano H, Sakon M, Wada H, Eguchi H, Kondo M. Partial contribution of tumour necrosis factor-related apoptosis-inducing ligand (TRAIL)/TRAIL receptor pathway to antitumor effects of interferon-alpha/5-fluorouracil against hepatocellular carcinoma. *Clin Cancer Res* 2004;**10**:7884–95.
10. Kondo M, Yamamoto H, Nagano H, Okami J, Ito Y, Shimizu J. Increased expression of COX-2 in nontumor liver tissue is associated with shorter disease-free survival in patients with hepatocellular carcinoma. *Clin Cancer Res* 1999;**5**:4005–12.
11. Capurro M, Wanless IR, Sherman M, Deboer G, Shi W, Miyoshi E. Glypican-3: a novel serum and histochemical marker for hepatocellular carcinoma. *Gastroenterology* 2003;**125**:89–97.
12. Zhang H, Ozaki I, Mizuta T, Yoshimura T, Matsuhashi S, Hisatomi A. Mechanism of beta 1-integrin-mediated hepatoma cell growth involves p27 and S-phase kinase-associated protein 2. *Hepatology* 2003;**38**:305–13.
13. Mottet D, Dumont V, Deccache Y, Demazy C, Ninane N, Raes M. Regulation of hypoxia-inducible factor-1alpha protein level during hypoxic conditions by the phosphatidylinositol 3-kinase/Akt/glycogen synthase kinase 3beta pathway in HepG2 cells. *J Biol Chem* 2003;**278**:31277–85.
14. Puisieux A, Ji J, Ozturk M. Annexin II up-regulates cellular levels of p11 protein by a post-translational mechanisms. *Biochem J* 1996;**313**:51–5.
15. Zobiack N, Gerke V, Rescher U. Complex formation and submembranous localization of annexin 2 and S100A10 in live HepG2 cells. *FEBS Lett* 2001;**500**:137–40.
16. Hollywood K, Brison DR, Goodacre R. Metabolomics: current technologies and future trends. *Proteomics* 2006;**6**:4716–23.
17. Cantley LC. The phosphoinositide 3-kinase pathway. *Science* 2002;**296**:1655–7.
18. Mootha VK, Bunkenborg J, Olsen JV, et al. Integrated analysis of protein composition, tissue diversity, and gene regulation in mouse mitochondria. *Cell* 2003;**115**:629–40.
19. Ye QH, Qin LX, Forgues M, He P, Kim JW, Peng AC. Predicting hepatitis B virus-positive metastatic hepatocellular carcinomas using gene expression profiling and supervised machine learning. *Nat Med* 2003;**9**: 416–23.
20. Hu DD, Lin EC, Kovach NL, Hoyer JR, Smith JW. A biochemical characterization of the binding of osteopontin to integrins alpha v beta 1 and alpha v beta 5. *J Biol Chem* 1995;**270**: 26232–8.
21. Song HH, Shi W, Filmus J. OCI-5/rat glypican-3 binds to fibroblast growth factor-2 but not to insulin-like growth factor-2. *J Biol Chem* 1997;**272**:7574–7.
22. Moorehead RA, Sanchez OH, Baldwin RM, Khokha R. Transgenic overexpression of IGF-II induces spontaneous lung tumors: a model for human lung adenocarcinoma. *Oncogene* 2003;**22**:853–7.
23. Regl G, Kasper M, Schnidar H, Eichberger T, Neill GW, Ikram MS. The zinc-finger transcription factor GLI2 antagonizes contact inhibition and differentiation of human epidermal cells. *Oncogene* 2004;**23**:1263–74.
24. Apte U, Zeng G, Muller P, Tan X, Micsenyi A, Cieply B. Activation of Wnt/beta-catenin pathway during hepatocyte growth factor-induced hepatomegaly in mice. *Hepatology* 2006;**44**:992–1002.
25. Gerke V, Moss SE. Annexins: from structure to function. *Physiol Rev* 2002;**82**:331–71.
26. Yamada A, Irie K, Hirota T, Ooshio T, Fukuhara A, Takai Y. Involvement of the annexin II-S100A10 complex in the formation of E-cadherin-based adherens junctions in Madin–Darby canine kidney cells. *J Biol Chem* 2005;**280**: 6016–27.
27. Kovacs EM, Ali RG, McCormack AJ, Yap AS. E-cadherin homophilic ligation directly signals through Rac and phosphatidylinositol 3-kinase to regulate adhesive contacts. *J Biol Chem* 2002;**277**:6708–18.
28. Siu MK, Wong CH, Lee WM, Cheng CY. Sertoli-germ cell anchoring junction dynamics in the testis are regulated by an interplay of lipid and protein kinases. *J Biol Chem* 2005;**280**:25029–47.
29. Abenoza P, Manivel JC, Wick MR, Hagen K, Dehner LP. Hepatoblastoma: an immunohistochemical and ultrastructural study. *Hum Pathol* 1987;**18**: 1025–35.
30. Moinzadeh P, Breuhahn K, Stutzer H, Schirmacher P. Chromosome alterations in human hepatocellular carcinomas correlate with aetiology and histological grade–results of an explorative CGH meta-analysis. *Br J Cancer* 2005;**92**:935–41.

**British Journal of Cancer (2008) 99,** 1307–1315

**www.bjcancer.com**

# Integrative approach for differentially overexpressed genes in gastric cancer by combining large-scale gene expression profiling and network analysis

**A Takeno[1], I Takemasa[*,1], Y Doki[1], M Yamasaki[1], H Miyata[1], S Takiguchi[1], Y Fujiwara[1], K Matsubara[2] and M Monden[1]**

*[1]Department of Surgery, Graduate School of Medicine, Osaka University, 2-2 Yamadaoka Suita, Osaka 565-0871, Japan; [2]DNA Chip Research Inc., 1-1-43 Suehirocho, Tsurumi, Yokohama, Kanagawa 230-0045, Japan*

Gene expression profiling is a valuable tool for identifying differentially expressed genes in studies of disease subtype and patient outcome for various cancers. However, it remains difficult to assign biological significance to the vast number of genes. There is an increasing awareness of gene expression profile as an important part of the contextual molecular network at play in complex biological processes such as cancer initiation and progression. This study analysed the transcriptional profiles commonly activated at different stages of gastric cancers using an integrated approach combining gene expression profiling of 222 human tissues and gene regulatory dynamic mapping. We focused on an inferred core network with *CDKN1A* ($p21^{WAF1/CIP1}$) as the hub, and extracted seven candidates for gastric carcinogenesis (*MMP7, SPARC, SOD2, INHBA, IGFBP7, NEK6, LUM*). They were classified into two groups based on the correlation between expression level and stage. The seven genes were commonly activated and their expression levels tended to increase as disease progressed. NEK6 and INHBA are particularly promising candidate genes overexpressed at the protein level, as confirmed by immunohistochemistry and western blotting. This integrated approach could help to identify candidate players in gastric carcinogenesis and progression. These genes are potential markers of gastric cancer regardless of stage.
*British Journal of Cancer* (2008) **99,** 1307–1315. doi:10.1038/sj.bjc.6604682 www.bjcancer.com
Published online 30 September 2008


**Keywords:** gastric cancer; gene expression profiling; network mapping; focus genes; common gene activation; integrative approach

Gastric cancer remains a major cause of cancer deaths worldwide despite early detection and curative surgery. Prognosis is favourable in early-stage disease with 5-year survival rates of 90% reported following gastrectomy and lymph node dissection. In contrast, patients diagnosed with advanced-stage cancer have 5-year survival rates of 20–30%, and the overall poor survival outcome for gastric cancer is attributed to these patient populations (Dicken *et al*, 2005). An efficient system for detecting disease status in gastric cancer regardless of its clinical stage is clearly needed to improve overall survival.

Gastric cancer is routinely classified according to the tumour-node-metastasis parameters of the primary tumour, lymph nodes, and metastasis. This classification helps the clinician to stage the tumour and develop a management strategy, as well as to provide an indication of prognosis. However, this conventional classification is not strong enough to predict individual prognosis, rendering uniform adjuvant therapy of limited value because of unnecessary adverse events. The use of molecular markers or gene profiling coupled with multivariate predictive models is designed to attain more accurate prognostic models. Recent molecular analyses revealed that gastric cancers closely associate with alterations in several interesting genes, such as p53 (Tamura *et al*, 1991; Uchino *et al*, 1993), p21 (Czerniak *et al*, 1989), c-met (Kaji *et al*, 1996), TGF-$\beta$ (Park *et al*, 1994; Nakamura *et al*, 1998), and $\beta$-catenin (Park *et al*, 1999). However, these single candidate molecules yield different results among studies and the available data are unconvincing. Thus, the potential use of combinations of multiple markers instead of a single marker has been previously commented upon for the understanding of cancer biology or the prediction of patient prognosis (Lee *et al*, 2007).

The past decade has seen a revolution in high-throughput technologies for molecular profiling in cancer research. Particularly, gene expression profiling has enabled researchers to quantify biological states and consequently uncover subtle phenotypes important in cancer. Such analyses of tumour tissues have provided unique opportunities to develop profiles that can distinguish, identify, and classify discrete subsets of disease, predict the disease outcome, and even predict the response to therapy (Golub *et al*, 1999; Perou *et al*, 2000; van 't Veer *et al*, 2002; van de Vijver *et al*, 2002; Pittman *et al*, 2004). For example, expression profiling in gastric cancer identified novel target molecules involved in gastric carcinogenesis by comparing cancerous and healthy tissues (Boussioutas *et al*, 2003; Kim *et al*, 2003, 2005).

Despite their potential power, gene expression profiling has major limitations. Interpreting the significance of identified genes

*Correspondence: Dr I Takemasa;
E-mail: itakemasa@gesurg.med.osaka-u.ac.jp
Received 17 April 2008; revised 18 August 2008; accepted 28 August 2008; published online 30 September 2008

without any unifying biological theme can be difficult, makeshift, and dependent on the biologist's area of expertise. It is frequently challenging to understand a specific regulatory network involving enormous numbers of proteins. Furthermore, an approach that ignores biological cues may generate poor reproducibility among different studies of the same biological system. To overcome these analytical challenges, several recent studies have focused on phenotypic analysis of primary tumours using gene expression profiling, with a view to further understanding the roles of signalling pathways deregulated by the oncogenic process (Rhodes and Chinnaiyan, 2005; Rhodes *et al*, 2005).

This study sought to identify transcriptional profiles commonly activated across a wide range of stages in gastric cancer, as well as core networks in gastric carcinogenesis. It used an integrated approach combining gene expression profiling of over 200 human tissues with dynamic gene mapping. We identified seven candidates among the network that reflected essential transcriptional features of neoplastic transformation and progression, and validated these quantitatively by real-time reverse transcription (RT)-PCR. We also evaluated the expression of the encoded proteins in gastric cancer tissues by immunohistochemistry and western blotting, and identified novel potential markers for detecting gastric cancers.

## MATERIALS AND METHODS

### Tissue samples

Samples were obtained from 222 patients with gastric cancer who underwent curative resection at the following institutions: Osaka University Hospital, National Osaka Hospital, Osaka Medical Center for Cancer and Cardiovascular Diseases, Sakai Municipal Hospital, Toyonaka Municipal Hospital, Mino Municipal Hospital, NTT West Osaka Hospital, Kinki Central Hospital, Suita Municipal Hospital, and Kansai Rosai Hospital. None of the patients received chemotherapy or radiotherapy before surgery. Tissues were evaluated macroscopically and microscopically according to the general rules for gastric cancer study in surgery and pathology in Japan. All cancers showed a depth of invasion beyond the subserosa. The clinical and pathological features are listed in Table 1. All aspects of our study protocol were performed according to the ethical guidelines set by the committee of the three Ministries of the Japanese Government, and each subject provided informed consent.

### Extraction of RNA and quality assessment

The tumour specimens were cut into pieces (approximately 8 $mm^3$) within 2 h after surgical resection and stored in RNAlater™ (Ambion, Austin, TX) at −80°C until use. Total RNA was purified from clinical samples using TRIzol reagent (Invitrogen, San Diego, CA, USA) according to the protocol supplied by the manufacturer. RNA integrity was assessed using an Agilent 2100 Bioanalyzer and RNA 6000 LabChip kits (Yokokawa Analytical Systems, Tokyo, Japan). Only high-quality RNAs with intact 18S and 28S sequences were used for the subsequent analysis. Fifteen RNA samples extracted from normal gastric epithelium were mixed as a reference control.

**Table 1** Clinical and pathological features of 222 patients

| | |
|---|---|
| Age (years) median (range) | 68 (23–92) |
| Sex (male/female) | 156:66 |
| *Location* | |
| Upper | 62 |
| Middle | 70 |
| Lower | 90 |
| *Histopathological type* | |
| Differentiated | 102 |
| Undifferentiated | 120 |
| *Pathological stage* | |
| I | 30 |
| II | 58 |
| III | 81 |
| VI | 53 |

### Preparation of fluorescently labelled aRNA targets and hybridisation

Extracted RNA samples were amplified with T7 RNA polymerase using the Amino Allyl MessageAmp™ aRNA kit (Ambion) according to the protocol provided by the manufacturer. The quality of each Amino Allyl-aRNA sample was checked on the Agilent 2100 Bioanalyzer. Five μg of control and experimental aRNA samples were labelled with Cy3 and Cy5, respectively, mixed, and then hybridised on an oligonucleotide microarray covering 30 000 human probes (AceGene Human 30K; DNA Chip Research and Hitachi Software Engineering Co, Yokohama, Japan). The experimental protocol is available at http://www.dna-chip.co.jp/thesis/AceGeneProtocol.pdf. The microarrays were scanned using a ScanArray 4000 (GSI Lumonics, Billerica, MA, USA).

### Analysis of microarray data

Signal values were calculated by DNASISArray software (Hitachi, Tokyo). Following background subtraction, data with low signal intensities were excluded from additional investigation. In each sample, the Cy5/Cy3 ratio values were log-transformed and globally equalised to remove deviation of the signal intensity between whole Cy3- and Cy5-fluorescence by subtracting the median of all log (Cy5/Cy3) values from each log (Cy5/Cy3) value. Supplementary information is available on our website (http://www.dna-chip.co.jp/).

### Network analysis

The Ingenuity Pathway (INGP) analysis was used to depict several networks in gastric cancer. The INGP software is a web-delivered application that enables biologists to discover, visualise, and explore therapeutically relevant networks significant to gene expression data sets. A detailed description of INGP analysis is available at Ingenuity Systems website (http//www.ingenuity.com). The average $\log_2$ expression values were used to calculate the fold change between gastric cancer and normal epithelium. The data set containing gene identifiers and their corresponding expression values were then uploaded into the INGP as a tab-delimited text file for analysis. Each gene identifier was mapped to its corresponding gene object in the Ingenuity Pathway Knowledge Base.

To understand how the genes identified by inferential statistics are related as focus genes, we uploaded the target genes into the Ingenuity Knowledge Base and generated several networks. On the basis of focus genes, new and expanded pathway maps, connections, and specific gene-gene interactions were inferred, functionally analysed, and used to build on the existing pathway knowledge base. To generate networks, the knowledge base was queried for interactions between focus genes and all other gene objects stored therein. The output, displayed graphically as nodes (genes) and edges (the biological relationship between the nodes), represented a significantly consistent number of biological pathways and functions implicated by the empirical data sets.

### RT reaction

Complementary DNAs (cDNAs) were generated with avian myeloblastosis virus reverse transcriptase (Promega, Madison, WI, USA) using the protocol recommended by the manufacturer. Briefly, 1 $\mu$g of RNA was mixed with RT reagents including oligo-$(dT)_{15}$ primer and incubated at 42°C for 15 min, followed by heating at 95°C for 5 min for enzyme inactivation.

### Quantitative RT-PCR with the LightCycler™

To validate the microaray data, quantitative PCR was performed using real-time PCR with a LightCycler (Idaho Tech, ID, USA). PCR reagents contained 1x LightCycler DNA Master SYBR Green I (Roche Diagnostics, Mannheim, Germany), 0.2 $\mu$M of each primer, 3 mM $MgCl_2$, and 2 $\mu$l of cDNA template. PCR conditions were as follows: one cycle of denaturing at 95°C for 10 min, followed by 40 cycles of 95°C for 15 s, 62°C for 5 s, and 72°C for 10 s. The housekeeping gene glyceraldehyde-3-phosphate dehydrogenase (*GAPDH*) was amplified quantitatively at the same time to verify the integrity of RNA and to improve the diagnostic quality of the technique. The intensity of fluorescence was calculated at each cycle and a standard curve was constructed with 10-fold serial dilutions of cDNA obtained from the mixture of normal gastric epitheliums. The primer sequences for PCR amplification are listed below: *MMP7* forward primer, 5′→GTCTCGGAGGAGATGC TCAC→3′ and reverse, 3′→GAGGAATGTCCCATACCC→5′; *SPARC* forward primer, 5′→CATTGACGGGTACCTCTCCC→3′ and reverse, 3′→CGATATCCTTCTGCTTGATGC→5′; *INHBA* forward primer, 5′→ATCATTGCTCCCTCTGGCTA →3′ and reverse, 3′→ ACGATTTGAGGTTGGCAAAG→5′; *IGFBP7* forward primer, 5′→AAGTAACTGGCTGGGTGCTG→3′ and reverse, 3′→TATAGCTCGGCACCTTCACC →5′; *NEK6* forward primer, 5′→TGTCTGCTGTACGAGATGGC→3′ and reverse, 3′→GATGC ACATGCTGACCAGTT→5′; *LUM* forward primer, 5′→GACATAA AGAGCTTCTGCAA→3′ and reverse, 3′→TTGTTCCAGGATA CAGATATT→5′; *SOD2* forward primer, 5′→GCAAGGAACA ACAGGCCTTA→3′ and reverse, 3′→CAGCATAACGATCGTG GTTT→5′; *GAPDH* forward primer, 5′→CAACTACATGGTTTAC ATGTTC →3′ and reverse, 3′→GCCAGTGGACTCC ACGAC →5′.

### Immunohistochemistry

Sections (3.5-$\mu$m thick) were deparaffinised in xylene and rehydrated. They were subjected to immunohistochemical analysis using the avidin-biotin-peroxidase complex (ABC) method with a Vectastain ABC-peroxidase kit (Vector Laboratories, Burlingame, CA, USA). The tissue sections were incubated overnight with the primary antibodies; anti-human INHBA (Serotec, Oxford, UK; 1:300 dilution) and anti-human NEK6 (GeneTex, San Antonio, TX; 1:200 dilution), at 4°C. Negative control staining was performed with the use of normal mouse or goat IgG instead of the primary antibody, yielding negative results in all patients.

### Western blotting

Frozen tumour and noncancerous tissues were homogenised in 0.5 ml radioimmunoprecipitation assay buffer (25 mmol $l^{-1}$ Tris (pH 7.4), 50 mmol $l^{-1}$ NaCl, 0.5% sodium deoxycholate, 2% NP40, and 0.2% SDS) containing protease inhibitors (1 mmol $l^{-1}$ phenylmethylsulfonyl fluoride, 10 $\mu$g $ml^{-1}$ aprotinin, and 10 $\mu$g $ml^{-1}$ leupeptin). The homogenate was centrifuged at 12 000 **g** for 20 min at 4°C. The resulting supernatant was collected and total protein concentration was determined using the Bradford protein assay (Bio-Rad, Hercules, CA, USA). Then, 100 $\mu$g of the total protein was premixed with loading buffer (0.05 mol $l^{-1}$ Tris-HCl (pH 6.8), 2% SDS, 0.2 mol $l^{-1}$ n-mercaptoethanol, 10% glycerol, and 0.001% bromophenol blue), boiled for 5 min, and subjected to SDS-PAGE on 10% gels. Proteins were then transferred onto polyvinylidene difluoride membrane (Boehringer Mannheim) using a transblot apparatus in a buffer containing 0.02 mol $l^{-1}$ Tris-HCl (pH 8.3), 0.2 mol $l^{-1}$ glycine, and 20% methanol. After blocking in 10% skim milk, the membrane was incubated overnight with anti-human INHBA (1:200 dilution), anti-human NEK6 (Abgent, San Diego, CA, USA; 1:500 dilution) at 4°C, or anti-actin (Sigma-Aldrich, St Louis, MO, USA; 1:1000 dilution) for 1 h at room temperature. After three washes each for 10 min with TBS (0.02 mol $l^{-1}$ Tris-HCl (pH 7.5) and 0.1 mol $l^{-1}$ NaCl) containing 0.2% Tween 20, the filter was incubated with secondary antibody at 1:1000 dilution. The protein bands were detected using the enhanced chemiluminescence detection system (Amersham, Arlington Heights, IL, USA) according to the instructions supplied by the manufacturer.

## RESULTS

### Analysis of microarray data

The gene expression profiles of 222 primary gastric cancers were analysed on a 30K oligonucleotide DNA microarray. Of the full gene sequences (29 638 expressed genes excluding control spots), 271 (0.9%) genes showed >1.5-fold change in differential expression in at least 100 samples. Among these 271 genes, 50 had been described previously in gastric cancers, whereas 187 genes were previously not described in gastric cancer and 34 genes were categorised into ESTs (expressed sequence tags).

### Network analysis

Analysis of the commonly overexpressed 271 genes using the Ingenuity Knowledge Base generated several networks that identified 203 genes as focus genes. The knowledge base generated 17 networks composed of focus genes and all other gene objects stored in the base (Table 2). On the basis of overlapping networks, network-5 was found to be central (Supplementary Figure 1). The centred network-5 (network-5 and close relevant networks) included a substantial number of genes already implicated in gastric carcinogenesis (Figure 1), with numerous focus genes connected by several neighbourhood genes. Furthermore, the network analysis mapped *CDKN1A* ($p21^{WAF1/CIP1}$) to the core of the centred network-5, acting as a hub by interacting with surrounding focus genes. *CDKN1A* is associated with disease progression and prognosis in gastric cancer (Czerniak *et al*, 1989; Kasper *et al*, 1998).

We selected seven focus genes showing >2-fold change in differential expression for further analysis. Three of these are known to be involved in gastric cancer: *MMP7* (Yamashita *et al*, 1998), *SPARC* (Wang *et al*, 2004), and *SOD2* (Janssen *et al*, 2000), and the other four have no such reported associations (*INHBA, IGFBP7, NEK6,* and *LUM*).

### Correlation between activation of candidate gene and pathological stage

To assess the clinical significance of each and common activation of the seven genes, we correlated microarray expression level and pathological stage. By comparing the expression level of each gene in early stage (stages I and II) and late stage (III and IV), we found that they could be classified into two groups: group 1 consisted of *MMP7, IGFBP7,* and *NEK6*; their expression levels correlated significantly with pathological stage ($P=0.0087$, 0.01, and 0.0085, respectively, Student's *t*-test) (Figure 2A–C), whereas the expression levels of genes of group 2 (*SOD2, SPARC, LUM, INHBA*) showed no such correlation ($P=0.25$, 0.6, 0.86 and 0.32, respectively, Student's *t*-test) (Figure 2E–H ). Interestingly, the mean

**Table 2** Seventeen networks identified in the data set

| ID | Molecules in network | Score | Focus molecules |
|---|---|---|---|
| 1 | AEBP1, Ap1, APOC1, APOC2, APOE, BCL2A1, BID, CCL20, COX2, COX3, CTSL1, GDF15, GLA, HSPE1, IL1, IL32, INDO, LDL, LTA, LY96, MEOX2, MGP, MMP1, NCOR-LXR-Oxysterol-RXR-9 cis RA, NFκB, NR4A2, PDGF, Rar, RIPK2, Rxr, SERPINF1, SOD2, STK10, TNF receptor, TNFSF13B | 45 | 26 |
| 2 | Akt, COL1A1, CSE1 L, CXCL10, CYR61, FAP, FBN1, Fibrin, FN1, IFN-γ, Igfbp, IGFBP7, INHBA, Integrin, ITGB2, LTBP2, MIF, MMP, MMP7, MMP9, MMP12, PCOLCE, PI3K, PLAUR, PRKAA1, SLC3A2, SPARC, SULF1, TGFβ, TGFBI, THBS1, THY1, TIMP1, VCAN, VEGF | 45 | 26 |
| 3 | ACP5, ACTN1, ADORA3, AGXT, AIF1, CEBPB, CKS1B, CLEC4E, COL10A1, COL1A2, COL3A1, CREB, CREM, Cyclin A, Cyclin E, DNAJA1, E2f, ERK1/2, Histone h3, HLA-DPA1, HLA-DPB1, IFITM3, MAPK, MHC2α, PCNA, PKA, PTTG1, RFC4, SKP2, SPP1, STMN1, TGFBR1, UBE2C, Vitamin D3-VDR-RXR, ZNF160 | 43 | 25 |
| 4 | C13ORF15, CACYBP, CDC2, CDKN3, COL4A1, FCER1G, FCGR2A, FCGR2B, FCGR3A, FOXM1, FPR1, GZMB, HOMER1, IGE, JNK, LAMA4, LAMB1, LAMC1, LGALS1, MAD2L1, MEK, MEK1/2, NFAT, P38 MAPK, PKC(s), PLA2G7, Rac, RAN, RANBP1, Ras, RGS1, Rsk, SRGN, TCR, UBD | 41 | 24 |
| 5 | Ap1, BUB3, CDKN1A, CKS1B, CKS2 (includes EG:1164), CLEC2B, E2F4, epinephrine, F9, fructose-2,6-diphosphate, GCNT1, HMCN1 (includes EG:83872), HMGB3, HSPE1, IGF1R, IL15, INS1, KIAA0101, LGALS3BP, LUM, MAD2L1, NEK6, NPHS2, PBK, PDCD5, RPS21, S100A11 (includes EG:6282), SOD2, SPAG5, SPARC, ST8SIA1, STMN1, UBE2T, VKORC1, ZNF84 | 31 | 20 |
| 6 | Actin, ASB2, ATP6, ATP2B1, ATP5E, ATP6V1F, Caspase, CD163, Ck2, CLNS1A, F Actin, GEMIN5, H+-transporting two-sector ATPase, Insulin, JUB, LMNA, NEXN, PDGF BB, PFDN1, PFDN2, PFDN4, PFDN6, PLC, POLR2K, RNA polymerase II, RNU1B, S100A11 (includes EG:6282), SNRPD1, SNRPE, SNRPF, SNRPG, TCEB1, Ubiquitin, UCHL1, VBP1 | 27 | 18 |
| 7 | ACP5, ARF4, BUB1 (includes EG:699), C1ORF164, C20ORF24, CCR6, CCT3, CCT4, CCT5, CCT7, CCT8, CCT6A, CPNE3, CTSB, CTSK, DAPK1, DEFB103A, EBNA1BP2, FCGR3A, FGFR, HTRA1, IFI30, IL4, IL10RA, ITGB7, keratan sulphate, MBP, MRPS10, MYL6, NAB2, NNMT, PRSS3 (includes EG:5646), TFF3, TGFB1, TUBA1A | 27 | 18 |
| 8 | CDK10, GBP4 (includes EG:115361), GPNMB, GPR109B, HLA-DPB1, HLA-DRA, IFI30, IFITM1, IFNα, IFNβ, IFNAR1, IFNB1, IFNG, IFNK, ILF3, KIR2DL3, KIR2DS2, POMP, PTEN, PTP4A3, RARRES1, retinoic acid, RFX1, RFX5, RFXANK, RFXAP, RPS19, RPS20, SERPINA5, STX5, TBCB, TMSB10, TREM2, TREM3, TRIM22, TYROBP | 25 | 17 |
| 9 | CKLF, CLDN16, F2, GABRD, GGH, LAMP1, LAMP2, LEPRE1, MYC, MYCN, PAICS, PRDM5, Proteasome PA700/20s, PSMA, PSMA1, PSMA2, PSMA4, PSMA5, PSMA6, PSMA7, PSMB1, PSMB2, PSMB3, PSMB4, PSMB5, PSMB6, PSMB7, PSMD6, PSMD14, RPL31, RPL37, RPS19, RPS20, RPS27, TUBA1B | 19 | 14 |
| 10 | β-estradiol, BTK, dihydrotestosterone, EXOC1, EXOC2, EXOC3, EXOC5, EXOC7, EXOC8, FGF7, FGFR2, FSHB, GTP, GUCY1A3, INPP5F, ITGBL1, MLLT1, MME, NFE2L3, NME1, NME2, NUDT1, phosphatidylinositol-3,4,5-trisphosphate, PIB5PA, PRUNE, RAP1B, RND3, RRAD, SEC61G, SFRP2, SLC7A8, SLCO3A1, SPARC, TMEPAI, VHL | 17 | 13 |
| 11 | ABCB4, ACO1, ASXL1, ASXL2, ASXL3, C7ORF24, CBX2, CDKN2A, COL1A1, EZH2, FOS, FST, FTH1, FTL, FTMT, GAL, GNRHR, HIF1A, HIG2, iron, KNG1 (includes EG:3827), LOX, MELK, MYH4, NTF3, PCGF1, PCGF6, PCNX, PDGF Ab, PHF1, PHF19, progesterone, RPS6, SFRP4, TGFBI | 12 | 10 |
| 12 | ATP9B, $Mg^{2+}$-ATPase | 2 | 1 |
| 13 | *N*-acetylglucosaminylphosphatidylinositol deacetylase, PIGL | 2 | 1 |
| 14 | Mrlc, MYLIP | 2 | 1 |
| 15 | EXOSC4, LRRC8D | 2 | 1 |
| 16 | GDP-Gnat2-Gngt2-Transducin β (cone), GNGT2, Gngt2-transducin beta (cone) | 2 | 1 |
| 17 | ADP-D-mannose, ADP-D-ribose, ADP-sugar diphosphatase, ADPribose diphosphatase, AMP, D-ribose-5-phosphate, nucleoside-diphosphatase, NUDT5 | 1 | 1 |

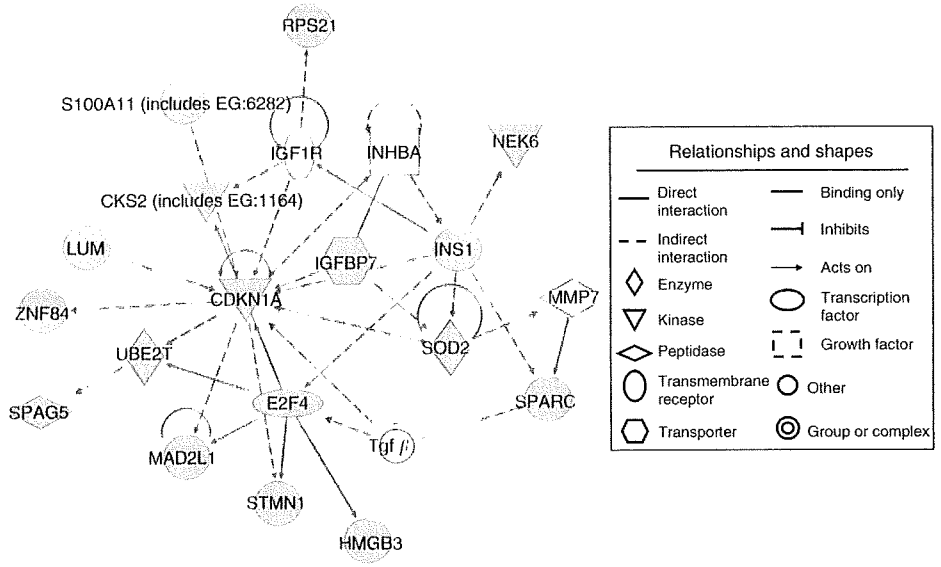


**Figure 1** Inferential core network (network-5 and its close relevant networks) comprising many focus genes and several neighbourhood genes that connect the focus genes. Greyed nodes are part of network-5.

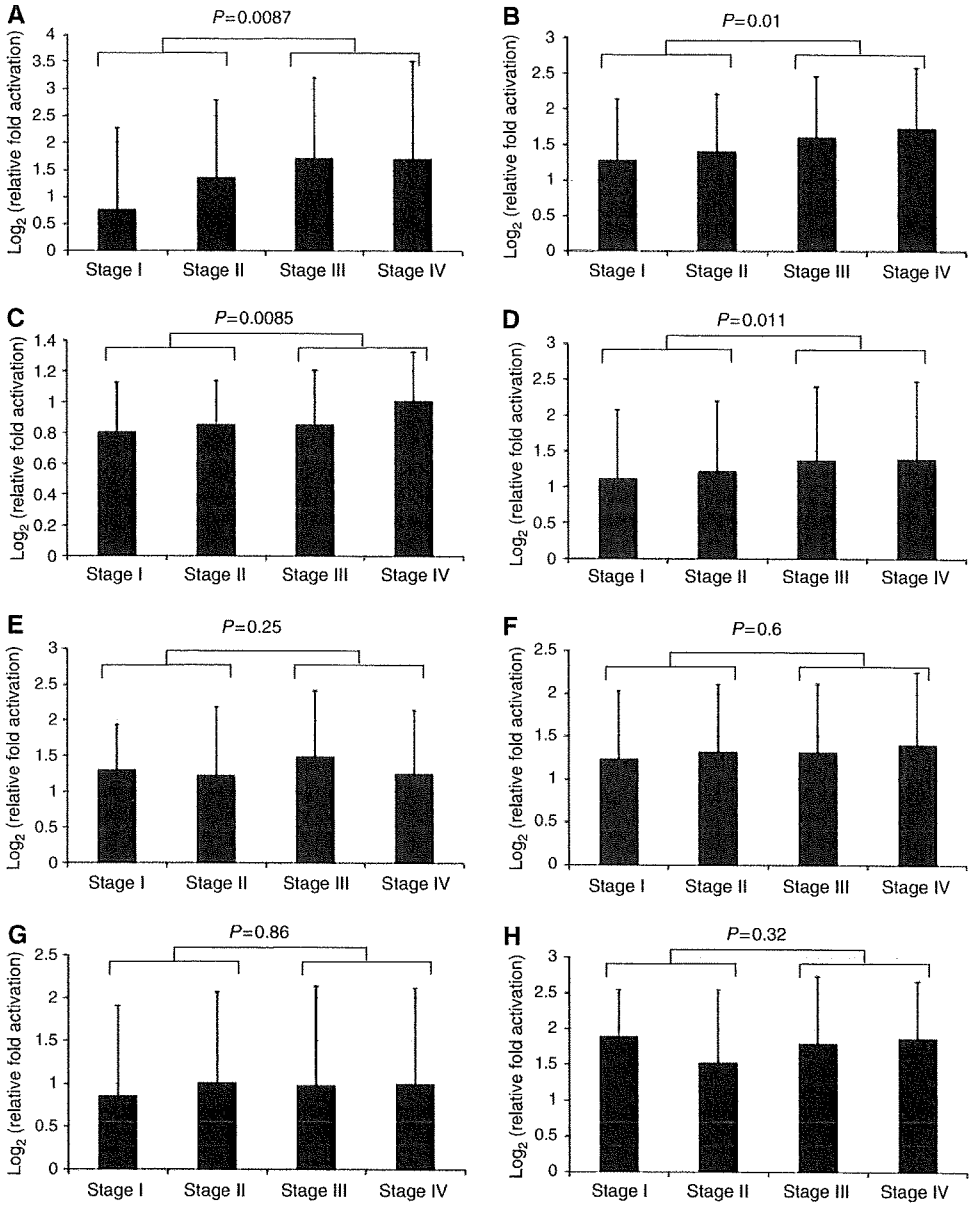


**Figure 2** Correlation between activation of each candidate gene and pathological stage ($n = 222$). The expression levels of genes of group 1 ((**A**) *MMP7*, (**B**) *IGFBP7*, (**C**) *NEK6*) correlated significantly with pathological stage ($P = 0.0087$, 0.01, and 0.0085, respectively). The mean expression of the seven genes also correlated with pathological stage ($P = 0.011$) (**D**). The expression levels of genes of group 2 ((**E**) *SOD2*, (**F**) *SPARC*, (**G**) *LUM*, (**H**) *INHBA*) did not correlate significantly with pathological stage ($P = 0.25$, 0.6, 0.86, and 0.32, respectively).

expression of the seven genes correlated with the pathological stage ($P = 0.011$) (Figure 2D).

## Validation of mRNA levels for selected genes using quantitative RT-PCR

To provide further quantitative validation of our microarray data for the 7 genes, we analysed 13 test tumour samples by quantitative RT-PCR and compared the results with the quantified mRNA expression levels on the microarray (Figure 3). All 7 genes were highly expressed across the 13 cancers and the microarray data agreed with those obtained by quantitative RT-PCR. Similar agreement was found in a subsequent comparative analysis of 14 validation tumour samples (Figure 3). We also compared the expression of the candidate genes with the mean expression level of the corresponding genes in 8 normal tissues that were used for microarray reference control. The results showed upregulation of each candidate gene compared with that in the normal tissues (Figure 3).

## Protein expression of selected genes by immunohistochemistry and western blotting

Finally, we tested the encoded protein expression for each identified focus gene using immunohistochemistry and western blotting. Immunohistochemistry showed high expression of INHBA and NEK6 proteins in 14 of 20 and 24 of 27 tumour tissues, respectively (Figure 4A–D), whereas IGFBP7 and LUM

proteins showed little immunoreactivity in tumour tissue relative to adjacent healthy tissue (data not shown). Each of these proteins was expressed in >50% cells in each tissue examined and all were localised into the cytoplasm.

Western blotting showed strong bands for both NEK6 and INHBA in gastric cancer tissues compared to normal tissue in all three pairs (Figure 4E).

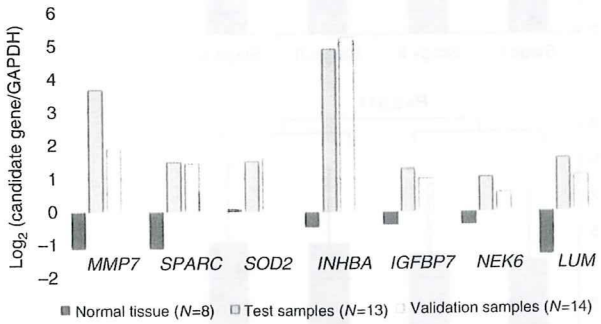


**Figure 3** Bar chart shows mRNA levels of candidate genes using quantitative reverse transcription–PCR in normal gastric tissue ($n=8$, microarray reference control), test samples ($n=13$), and validation samples ($n=14$). Data are mean expression level of candidate gene relative to that of GAPDH in the examined tissues.

## DISCUSSION

Comprehensive gene expression profiling is a useful tool for analysing several thousands of genes in multiple samples simultaneously. In gastric cancer, this approach successfully discriminated cancerous and noncancerous tissues (Hippo *et al*, 2002). Since then, several studies have searched for novel genes related to carcinogenesis of gastric cancer and novel clinical subtypes related to biological malignancy using comprehensive gene expression profiling (Hasegawa *et al*, 2002; Ji *et al*, 2002; Boussioutas *et al*, 2003; Kim *et al*, 2003, 2005; Oien *et al*, 2003; Jinawath *et al*, 2004; Motoori *et al*, 2005). However, these data were generally obtained from human cell lines or small-scale tissue samples. Here, we analysed the gene expression profiles of more than 200 tissue samples covering every pathological stage, and verified the findings at both the mRNA and protein levels to increase the universality of our microarray data. Such a study is more likely to identify specific expression profiles that are commonly activated and thus more reflective of crucial transcriptional features of neoplastic transformation and progression in gastric cancers. In fact, increasing recognition that this large-scale, systematic approach is necessary to view the overall molecular events responsible for carcinogenesis has spawned several recent studies combining large-scale analysis of gene expression with knowledge-based and relevance network analysis (Bredel *et al*, 2005; Abdel-Aziz *et al*, 2007). Using such an approach also

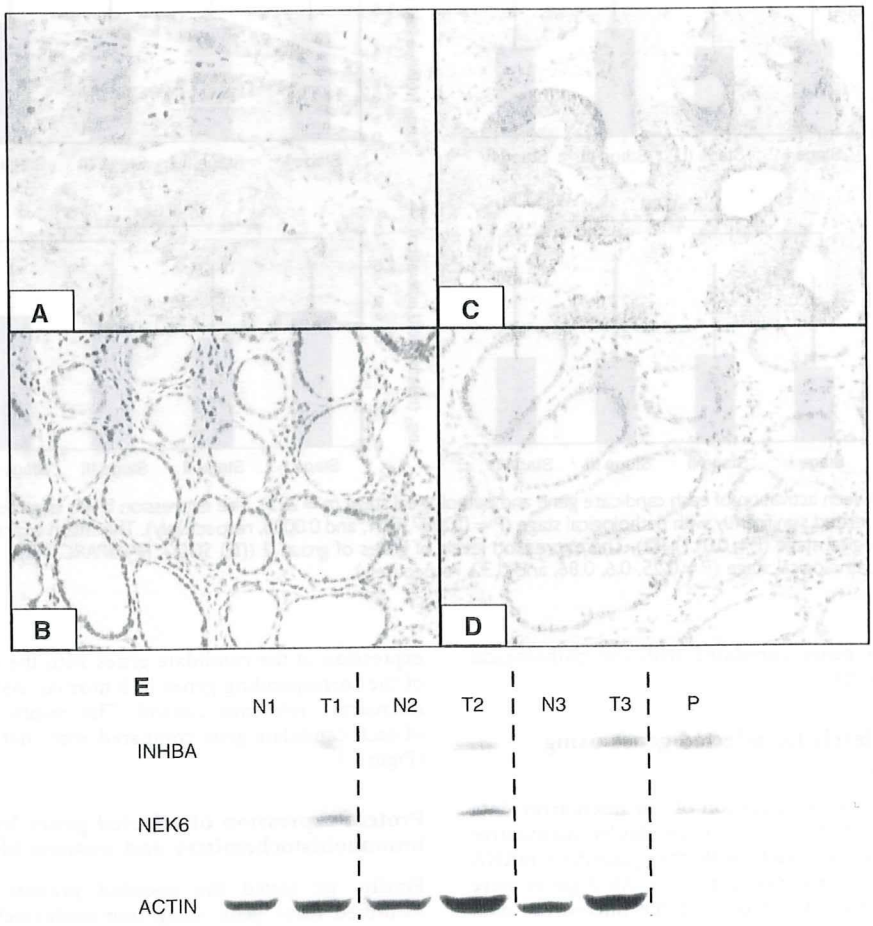


**Figure 4** (**A**–**D**) Representative images of immunostaining for INHBA and NEK6. (**A**) Tumour tissue expressing INHBA; (**B**) healthy tissue for INHBA; (**C**) tumour tissue expressing NEK6; (**D**) healthy tissue for NEK6. Magnification, × 200. (**E**) Western blotting analysis of INHBA and NEK6 in three pairs of tumour (T) and normal (N) tissues. Anti-$\beta$-actin was used as control for protein level. P, positive control tissue.

identified significantly upregulated genes linked to activated pathways as potential key molecules in hepatocellular carcinoma (Kittaka *et al*, 2008).

Dynamic mapping of 271 genes differentially expressed in gastric cancer tissues in this study revealed links among the majority of genes (203 genes, 84%) based on the Ingenuity Pathway Knowledge Base. This finding indicates that such gene populations do not act as individual units, but rather collaborate closely in overlapping networks during gastric carcinogenesis. Among the 17 networks identified here, network-5 was mapped to the centre of the overlapping network and contained the largest number of focus genes, implicating it as a key network. Furthermore, the identified networks assumed a cluster of robust genes implicated in gastric cancer-related genes. Our network analysis also revealed *CDKN1A* ($p21^{WAF1/CIP1}$) as a hub gene that links to a large number of nodes and possibly determines the fundamental behaviour of the network.

The clinical significance of activation of our seven selected genes was further investigated by correlating the microarray expression data with the pathological stage. As indicated in Figure 2, we found these genes could be classified into two groups: the expression levels of genes of group 1 (*MMP7, IGFBP7,* and *NEK6*), but not those of group 2 (*SOD2, SPARC, LUM* and *INHBA*), correlated significantly with pathological stage. This finding indicates that although genes of group 2 may be involved in tumour formation and survival, those of group 1 may be involved in tumour progression. Their common activation seems to serve gastric carcinogenesis and tumour survival regardless of the pathological stage, based on the finding of overexpression of all seven genes in all samples. Furthermore, the gradual increase in the mean expression with cancer stage suggests that these genes cooperate in tumour progression. These results strengthen our proposal that such candidate genes are commonly activated during gastric carcinogenesis.

We also analysed the expression of the seven candidate genes based on age, sex, location, and histopathological type. Although the expression levels of *MMP7, NEK6, SOD2, SPARC,* and *INHBA* did not correlate with any of the above factors, *IGFBP7* and *LUM* were significantly upregulated in undifferentiated tumours compared to differentiated tumours (data not shown). These results suggest the involvement of these genes in tumour differentiation.

We also postulated that these genes are regulated by complex linkage between specific signalling pathways such as cell cycle signalling and TGF-$\beta$ signalling, and that targeting several genes around *CDKN1A* ($p21^{WAF1/CIP1}$), which functions as a hub, can compensate each other. The differential expressions were also corroborated by quantitative RT–PCR data in some of the previously tested tissue samples and in 14 validation samples. Together, these findings implicate all seven genes in gastric carcinogenesis, including the four that were not previously related to human gastric cancer.

Transcript profiling studies require complementary protein analysis to fully understand the associated regulatory process in living organisms. By itself, profiling does not adequately reflect the fluctuating signalling events occurring at the proteomic level, based on the evidence that only a subset of proteins correlate significantly with mRNA abundance (Chen *et al*, 2002; Nishizuka *et al*, 2003; Tian *et al*, 2004). These seemingly anomalous results are explained partly by translational processes whereby microRNAs repress the translation of mRNA into proteins, and partly by post-translational modifications such as phosphorylation, methylation, acetylation, and ubiquitination. For that reason, the expression levels of proteins encoded by highly overexpressed genes related to gastric carcinogenesis require further investigation. This study detected protein expression for two gene products among the four previously noncancer-related genes. Furthermore, NEK6 protein was strongly stained in most of the cancer tissues, but showed less mRNA signal compared to the remaining six genes. This finding suggests that NEK6 might be significantly modified post-translationally.

Matrix metalloproteinases including MMP7 play important roles in determining tumour invasion and metastasis and *MMP7* gene expression correlates with vessel invasion and both lymphatic and hematogenous metastases (Yamashita *et al*, 1998). Increased SPARC expression is linked to advanced gastric cancer (Wang *et al*, 2004), although the expression of SOD2 (Mn-SOD; manganese superoxide dismutase) was significantly enhanced in cancer tissues compared with normal mucosa, and the Mn-SOD ratio was proposed as an independent prognostic parameter (Janssen *et al*, 2000). The *IGFBP7* gene was upregulated in diffuse-type gastric cancer (Boussioutas *et al*, 2003) and in 22 gastric cancer/nontumour mucosa paired tissues samples (Kim *et al*, 2003). Interestingly, recent study revealed that TGF-$\beta$ signalling including *INHBA* accounted for some of the main differences between normal tissue and gastric cancer at the transcript level (Yang *et al*, 2007).

As stated, this study identified several genes, such as LUM and NEK6, which were not previously associated with human gastric cancer. LUM is a member of the small leucine-rich proteoglycan family that induces apoptosis and suppresses cell proliferation. Its reduced expression has been associated with poor outcome in invasive carcinoma (Vuillermoz *et al*, 2004; Schuetz *et al*, 2006). NIMA (never in mitosis, gene A) was originally identified in *Aspergillus nidulans* as a serine/threonine kinase critical for cell cycle progression (Osmani *et al*, 1988). Human NIMA-related kinases (Neks) have high homology to NIMA in the N-terminal catalytic domain sequences. *NEK6* is a Neks-family gene required for mitotic progression in human cells (Roig *et al*, 2002). Inhibition of *NEK6* by either overexpression of an inactive *NEK6* mutant or elimination of endogenous *NEK6* using siRNA-arrested cells in M phase and triggered apoptosis (Belham *et al*, 2003; Yin *et al*, 2003). A recent study demonstrated overexpression of *NEK6* transcripts in hepatocellular carcinoma (Chen *et al*, 2006), although it was found to be frequently expressed among 125 serine/threonine kinase genes implicated in breast cancer, colorectal cancer, lung cancer, and laryngeal cancer by *in situ* hybridisation (Capra *et al*, 2006). However, no previous studies have shown *NEK6* expression in gastric cancers or NEK6 protein expression in any cancerous tissues. In data not shown here, we also found higher levels of NEK6 protein in advanced cancer compared to early-stage samples by immunohistochemistry.

In conclusion, this study used an integrated approach combining gene expression profiling and dynamic mapping of gene expression data on large sample numbers to identify novel candidate genes that may contribute to gastric carcinogenesis. The identified genes were universally validated in additional samples. In particular, NEK6 and INHBA are promising potential markers of gastric cancer regardless of disease stage.

## ACKNOWLEDGEMENTS

We thank the following physicians for providing the surgical specimens used in this study: Dr Motohiro Hirao from the National Osaka Hospital, Dr Kentaro Kishi from the Osaka Medical Center for Cancer and Cardiovascular Diseases, Dr Hiroshi Imamura from the Sakai Municipal Hospital, Dr Junya Fujita from the Toyonaka Municipal Hospital, Dr Shohei Iijima from the Mino Municipal Hospital, Dr Yutaka Kimura from the NTT West Osaka Hospital, Dr Ko Takachi from the Kinki Central Hospital, Dr Kentaro Maruyama from the Suita Municipal Hospital, and Dr Hirofumi Miki from the Kansai Rosai Hospital.

Supplementary Information accompanies the paper on British Journal of Cancer website (http://www.nature.com/bjc)

## REFERENCES

Abdel-Aziz HO, Takasaki I, Tabuchi Y, Nomoto K, Murai Y, Tsuneyama K, Takano Y (2007) High-density oligonucleotide microarrays and functional network analysis reveal extended lung carcinogenesis pathway maps and multiple interacting genes in NNK [4-(methylnitrosamino)-1-(3-pyridyle)-1-butanone] induced CD1 mouse lung tumor. *J Cancer Res Clin Oncol* **133:** 107–115

Belham C, Roig J, Caldwell JA, Aoyama Y, Kemp BE, Comb M, Avruch J (2003) A mitotic cascade of NIMA family kinases. Nercc1/Nek9 activates the Nek6 and Nek7 kinases. *J Biol Chem* **278:** 34897–34909

Boussioutas A, Li H, Liu J, Waring P, Lade S, Holloway AJ, Taupin D, Gorringe K, Haviv I, Desmond PV, Bowtell DD (2003) Distinctive patterns of gene expression in premalignant gastric mucosa and gastric cancer. *Cancer Res* **63:** 2569–2577

Bredel M, Bredel C, Juric D, Harsh GR, Vogel H, Recht LD, Sikic BI (2005) Functional network analysis reveals extended gliomagenesis pathway maps and three novel MYC-interacting genes in human gliomas. *Cancer Res* **65:** 8679–8689

Capra M, Nuciforo PG, Confalonieri S, Quarto M, Bianchi M, Nebuloni M, Boldorini R, Pallotti F, Viale G, Gishizky ML, Draetta GF, Di Fiore PP (2006) Frequent alterations in the expression of serine/threonine kinases in human cancers. *Cancer Res* **66:** 8147–8154

Chen G, Gharib TG, Huang CC, Taylor JM, Misek DE, Kardia SL, Giordano TJ, Iannettoni MD, Orringer MB, Hanash SM, Beer DG (2002) Discordant protein and mRNA expression in lung adenocarcinomas. *Mol Cell Proteomics* **1:** 304–313

Chen J, Li L, Zhang Y, Yang H, Wei Y, Zhang L, Liu X, Yu L (2006) Interaction of Pin1 with Nek6 and characterization of their expression correlation in Chinese hepatocellular carcinoma patients. *Biochem Biophys Res Commun* **341:** 1059–1065

Czerniak B, Herz F, Gorczyca W, Koss LG (1989) Expression of ras oncogene p21 protein in early gastric carcinoma and adjacent gastric epithelia. *Cancer* **64:** 1467–1473

Dicken BJ, Bigam DL, Cass C, Mackey JR, Joy AA, Hamilton SM (2005) Gastric adenocarcinoma: review and considerations for future directions. *Ann Surg* **241:** 27–39

Golub TR, Slonim DK, Tamayo P, Huard C, Gaasenbeek M, Mesirov JP, Coller H, Loh ML, Downing JR, Caligiuri MA, Bloomfield CD, Lander ES (1999) Molecular classification of cancer: class discovery and class prediction by gene expression monitoring. *Science* **286:** 531–537

Hasegawa S, Furukawa Y, Li M, Satoh S, Kato T, Watanabe T, Katagiri T, Tsunoda T, Yamaoka Y, Nakamura Y (2002) Genome-wide analysis of gene expression in intestinal-type gastric cancers using a complementary DNA microarray representing 23 040 genes. *Cancer Res* **62:** 7012–7017

Hippo Y, Taniguchi H, Tsutsumi S, Machida N, Chong JM, Fukayama M, Kodama T, Aburatani H (2002) Global gene expression analysis of gastric cancer by oligonucleotide microarrays. *Cancer Res* **62:** 233–240

Janssen AM, Bosman CB, van Duijn W, Oostendorp-van de Ruit MM, Kubben FJ, Griffioen G, Lamers CB, van Krieken JH, van de Velde CJ, Verspaget HW (2000) Superoxide dismutases in gastric and esophageal cancer and the prognostic impact in gastric cancer. *Clin Cancer Res* **6:** 3183–3192

Ji J, Chen X, Leung SY, Chi JT, Chu KM, Yuen ST, Li R, Chan AS, Li J, Dunphy N, So S (2002) Comprehensive analysis of the gene expression profiles in human gastric cancer cell lines. *Oncogene* **21:** 6549–6556

Jinawath N, Furukawa Y, Hasegawa S, Li M, Tsunoda T, Satoh S, Yamaguchi T, Imamura H, Inoue M, Shiozaki H, Nakamura Y (2004) Comparison of gene-expression profiles between diffuse- and intestinal-type gastric cancers using a genome-wide cDNA microarray. *Oncogene* **23:** 6830–6844

Kaji M, Yonemura Y, Harada S, Liu X, Terada I, Yamamoto H (1996) Participation of c-met in the progression of human gastric cancers: anti-c-met oligonucleotides inhibit proliferation or invasiveness of gastric cancer cells. *Cancer Gene Ther* **3:** 393–404

Kasper HU, Schneider-Stock R, Mellin W, Roessner A (1998) P21 protein expression and ras-oncogene mutations in gastric carcinoma: correlation with clinical data. *Int J Oncol* **12:** 69–74

Kim B, Bang S, Lee S, Kim S, Jung Y, Lee C, Choi K, Lee SG, Lee K, Lee Y, Kim SS, Yeom YI, Kim YS, Yoo HS, Song K, Lee I (2003) Expression profiling and subtype-specific expression of stomach cancer. *Cancer Res* **63:** 8248–8255

Kim JM, Sohn HY, Yoon SY, Oh JH, Yang JO, Kim JH, Song KS, Rho SM, Yoo HS, Kim YS, Kim JG, Kim NS (2005) Identification of gastric cancer-related genes using a cDNA microarray containing novel expressed sequence tags expressed in gastric cancer cells. *Clin Cancer Res* **11:** 473–482

Kittaka N, Takemasa I, Takeda Y, Marubashi S, Nagano H, Umeshita K, Dono K, Matsubara K, Matsuura N, Monden M (2008) Molecular mapping of human hepatocellular carcinoma provides deeper biological insight from genomic data. *Eur J Cancer* **44:** 885–897

Lee HS, Cho SB, Lee HE, Kim MA, Kim JH, Park do J, Kim JH, Yang HK, Lee BL, Kim WH (2007) Protein expression profiling and molecular classification of gastric cancer by the tissue array method. *Clin Cancer Res* **13:** 4154–4163

Motoori M, Takemasa I, Yano M, Saito S, Miyata H, Takiguchi S, Fujiwara Y, Yasuda T, Doki Y, Kurokawa Y, Ueno N, Oba S, Ishii S, Monden M, Kato K (2005) Prediction of recurrence in advanced gastric cancer patients after curative resection by gene expression profiling. *Int J Cancer* **114:** 963–968

Nakamura M, Katano M, Kuwahara A, Fujimoto K, Miyazaki K, Morisaki T, Mori M (1998) Transforming growth factor beta1 (TGF-beta1) is a preoperative prognostic indicator in advanced gastric carcinoma. *Br J Cancer* **78:** 1373–1378

Nishizuka S, Charboneau L, Young L, Major S, Reinhold WC, Waltham M, Kouros-Mehr H, Bussey KJ, Lee JK, Espina V, Munson PJ, Petricoin III E, Liotta LA, Weinstein JN (2003) Proteomic profiling of the NCI-60 cancer cell lines using new high-density reverse-phase lysate microarrays. *Proc Natl Acad Sci USA* **100:** 14229–14234

Oien KA, Vass JK, Downie I, Fullarton G, Keith WN (2003) Profiling, comparison and validation of gene expression in gastric carcinoma and normal stomach. *Oncogene* **22:** 4287–4300

Osmani SA, Pu RT, Morris NR (1988) Mitotic induction and maintenance by overexpression of a G2-specific gene that encodes a potential protein kinase. *Cell* **53:** 237–244

Park K, Kim SJ, Bang YJ, Park JG, Kim NK, Roberts AB, Sporn MB (1994) Genetic changes in the transforming growth factor beta (TGF-beta) type II receptor gene in human gastric cancer cells: correlation with sensitivity to growth inhibition by TGF-beta. *Proc Natl Acad Sci USA* **91:** 8772–8776

Park WS, Oh RR, Park JY, Lee SH, Shin MS, Kim YS, Kim SY, Lee HK, Kim PJ, Oh ST, Yoo NJ, Lee JY (1999) Frequent somatic mutations of the beta-catenin gene in intestinal-type gastric cancer. *Cancer Res* **59:** 4257–4260

Perou CM, Sorlie T, Eisen MB, van de Rijn M, Jeffrey SS, Rees CA, Pollack JR, Ross DT, Johnsen H, Akslen LA, Fluge O, Pergamenschikov A, Williams C, Zhu SX, Lonning PE, Borresen-Dale AL, Brown PO, Botstein D (2000) Molecular portraits of human breast tumours. *Nature* **406:** 747–752

Pittman J, Huang E, Dressman H, Horng CF, Cheng SH, Tsou MH, Chen CM, Bild A, Iversen ES, Huang AT, Nevins JR, West M (2004) Integrated modeling of clinical and gene expression information for personalized prediction of disease outcomes. *Proc Natl Acad Sci USA* **101:** 8431–8436

Rhodes DR, Chinnaiyan AM (2005) Integrative analysis of the cancer transcriptome. *Nat Genet* **37**(Suppl): S31–S37

Rhodes DR, Kalyana-Sundaram S, Mahavisno V, Barrette TR, Ghosh D, Chinnaiyan AM (2005) Mining for regulatory programs in the cancer transcriptome. *Nat Genet* **37:** 579–583

Roig J, Mikhailov A, Belham C, Avruch J (2002) Nercc1, a mammalian NIMA-family kinase, binds the Ran GTPase and regulates mitotic progression. *Genes Dev* **16:** 1640–1658

Schuetz CS, Bonin M, Clare SE, Nieselt K, Sotlar K, Walter M, Fehm T, Solomayer E, Riess O, Wallwiener D, Kurek R, Neubauer HJ (2006) Progression-specific genes identified by expression profiling of matched ductal carcinomas *in situ* and invasive breast tumors, combining laser capture microdissection and oligonucleotide microarray analysis. *Cancer Res* **66:** 5278–5286

Tamura G, Kihana T, Nomura K, Terada M, Sugimura T, Hirohashi S (1991) Detection of frequent p53 gene mutations in primary gastric cancer by cell sorting and polymerase chain reaction single-strand conformation polymorphism analysis. *Cancer Res* **51:** 3056–3058

Tian Q, Stepaniants SB, Mao M, Weng L, Feetham MC, Doyle MJ, Yi EC, Dai H, Thorsson V, Eng J, Goodlett D, Berger JP, Gunter B, Linseley PS, Stoughton RB, Aebersold R, Collins SJ, Hanlon WA, Hood LE (2004) Integrated genomic and proteomic analyses of gene expression in mammalian cells. *Mol Cell Proteomics* **3:** 960–969

Uchino S, Noguchi M, Ochiai A, Saito T, Kobayashi M, Hirohashi S (1993) p53 mutation in gastric cancer: a genetic model for carcinogenesis is common to gastric and colorectal cancer. *Int J Cancer* **54:** 759–764

van 't Veer LJ, Dai H, van de Vijver MJ, He YD, Hart AA, Mao M, Peterse HL, van der Kooy K, Marton MJ, Witteveen AT, Schreiber GJ, Kerkhoven

RM, Roberts C, Linsley PS, Bernards R, Friend SH (2002) Gene expression profiling predicts clinical outcome of breast cancer. *Nature* **415:** 530–536

van de Vijver MJ, He YD, van't Veer LJ, Dai H, Hart AA, Voskuil DW, Schreiber GJ, Peterse JL, Roberts C, Marton MJ, Parrish M, Atsma D, Witteveen A, Glas A, Delahaye L, van der Velde T, Bartelink H, Rodenhuis S, Rutgers ET, Friend SH, Bernards R (2002) A gene-expression signature as a predictor of survival in breast cancer. *N Engl J Med* **347:** 1999–2009

Vuillermoz B, Khoruzhenko A, D'Onofrio MF, Ramont L, Venteo L, Perreau C, Antonicelli F, Maquart FX, Wegrowski Y (2004) The small leucine-rich proteoglycan lumican inhibits melanoma progression. *Exp Cell Res* **296:** 294–306

Wang CS, Lin KH, Chen SL, Chan YF, Hsueh S (2004) Overexpression of SPARC gene in human gastric carcinoma and its clinic-pathologic significance. *Br J Cancer* **91:** 1924–1930

Yamashita K, Azumano I, Mai M, Okada Y (1998) Expression and tissue localization of matrix metalloproteinase 7 (matrilysin) in human gastric carcinomas. Implications for vessel invasion and metastasis. *Int J Cancer* **79:** 187–194

Yang S, Shin J, Park KH, Jeung HC, Rha SY, Noh SH, Yang WI, Chung HC (2007) Molecular basis of the differences between normal and tumor tissues of gastric cancer. *Biochim Biophys Acta* **1772:** 1033–1040

Yin MJ, Shao L, Voehringer D, Smeal T, Jallal B (2003) The serine/threonine kinase Nek6 is required for cell cycle progression through mitosis. *J Biol Chem* **278:** 52454–52460

# Overexpression of MT1-MMP is insufficient to increase experimental liver metastasis of human colon cancer cells

HIROFUMI YAMAMOTO[1], SHINGO NOURA[2], JIRO OKAMI[2], MAMORU UEMURA[1], ICHIRO TAKEMASA[1], MASATAKA IKEDA[1], HIDESHI ISHII[1], MITSUGU SEKIMOTO[1], NARIAKI MATSUURA[3], MORITO MONDEN[1] and MASAKI MORI[1]

[1]Department of Surgery, Gastroenterological Surgery, Graduate School of Medicine, Osaka University; [2]Department of Surgery, Osaka Medical Center for Cancer and Cardiovascular Diseases; [3]Department of Pathology, School of Allied Health Science, Faculty of Medicine, Osaka University, Osaka, Japan

Received June 13, 2008; Accepted August 1, 2008

DOI: 10.3892/ijmm_00000082

**Abstract.** The expression and activation of matrix metalloproteinases (MMPs) by tumor cells is correlated with invasive and metastatic potential. The purpose of this study was to examine the impact of increased membrane type 1 matrix metalloproteinase (MT1-MMP) expression on liver metastatic potential utilizing human colorectal cancer (CRC) cell lines. Three human CRC cell lines, DLD1, HCT116 and HT29, were stably transfected with the MT1-MMP cDNA, and experimental liver metastasis was established by injecting the cells into the spleens of nude mice. Reverse transcription-polymerase chain reaction (RT-PCR) confirmed increased expression of MT1-MMP mRNA in the stable tranfectants. *In vitro* analysis by gelatin zymography and morphological survey demonstrated that MT1-MMP transfectants displayed a matured gelatinolytic activity and invasive properties when cultured in 3D collagen gel, indicating that transduced MT1-MMP cDNA was functional. Although there was no difference in cell proliferation rate between MT1-MMP overexpressing cells and the Mock control cells, *in vivo* experiments indicated that the liver metastatic ability was not affected by MT1-MMP overexpression. Our findings indicated that conditional MT1-MMP overexpression was insufficient to increase experimental liver metastasis, suggesting a more complicated mechanism may be involved in the activation and regulation of MMPs cascades *in vivo*.

*Correspondence to*: Dr Hirofumi Yamamoto, Department of Surgery, Gastroenterological Surgery, Graduate School of Medicine, Osaka University, 2-2 Yamada-oka, Suita-City, Osaka 565-0871, Japan
E-mail: kobunyam@surg2.med.osaka-u.ac.jp

*Abbreviations:* CRC, colorectal cancer; ECM, extracellular matrix; FBS, fetal bovine serum; MT-1 MMP, membrane type 1 matrix metalloproteinase; RT, reverse transcription; PBGD, phorphobilinogen deaminase; PCR, polymerase chain reaction; TIMP, tissue inhibitors of matrix metalloproteinase

*Key words:* MT1-MMP, colorectal cancer, invasion, liver metastasis

## Introduction

Destruction of the extracellular matrix (ECM), especially the basement membrane, is an essential step in tumor invasion and metastasis. Degradation of the ECM generates a new avenue for invasion and allows movement of tumor cells across basement membrane. A major family of ECM degrading enzymes involved in this process is the matrix metalloproteinases (MMPs) family (1). MMPs are generally expressed at low level and induced in events that required ECM remodeling such as wound healing. Most MMPs are secreted in a latent form that requires proteolytic removal of the N-terminal propeptide to become catalytically active (2). These proteinases are regulated at transcription level and also at translation level and activated through induction of proteolytic cascades (3). Membrane-bound membrane type 1 matrix metalloproteinase (MT1-MMP) activates pro-MMP-2, which is shown to contribute to the invasive abilities of various tumors (4).

MT1-MMP, also termed MMP-14, is a transmembrane protein expressed in an active form (5). It cleaves or degrades various kinds of the ECM compounds including collagen, gelatin and fibrin and facilitates invasion and metastasis of tumor cells. MT1-MMP also activates several downstream MMPs, including the most widespread gelatinase, MMP-2 (gelatinase A) (6). There is evidence that mechanisms as diverse as autocatalytic processing, ectodomain shedding, homodimerization and internalization can all contribute to the modulation of MT1-MMP activity on the cell surface (3). The dynamic turnover of MT1-MMP at the migration edge by internalization is important for proper enzyme function during cell migration and invasion (7). MT1-MMP expression has been documented in several types of tumors and up-regulation of MT1-MMP is strongly implicated in tumor growth and metastasis spread (8-10). In colorectal cancer (CRC), MT1-MMP overexpression is noted during multi-stage tumorigenesis (11), and tumor phenotype stratified by

Table I. PCR primers.

| Gene | Sense primer | Antisense primer | Product size (bp) |
|---|---|---|---|
| MT1-MMP | 5'-ACCTACGTACCCACACACAG-3' | 5'-AAATTCTCCGTGTCCATCCA-3' | 661 |
| PBGD | 5'-AACGGCGGAAGAAAACAG-3' | 5'-TCCAATCTTAGAGAGTGCA-3' | 190 |

both MMP and tissue inhibitors of matrix metalloproteinase (TIMP) is associated with poor prognosis (12).

Since liver metastasis is one of the most frequent causes of death from CRC (13), we investigated whether MT1-MMP overexpression would contribute to facilitate formation of liver metastasis using 3 types of CRC cell lines stably tranfected with MT1-MMP cDNA. To our knowledge, this is the first study that investigated effects of MT1-MMP on liver metastatic potential using *in vivo* experimental liver metastasis model.

## Materials and methods

*Cell lines*. Three human CRC cell lines, namely DLD1, HCT119 and HT29 were obtained from the American Type Culture Collection (Manassas, VA). These cell were maintained in Dulbecco's modified Eagle's medium (DMEM) supplemented with 10% fetal bovine serum (FBS), 100 U/ml penicillin, and 100 $\mu$g/ml streptomycin in 5% $CO_2$ at 37°C.

*Expression plasmid and transfection*. MT1-MMP expression plasmid with neomycin resistance was kindly provided by Professor S. Weiss from University of Michigan (14,15). A pcDNA3 vector (Invitrogen, Carlsbad, CA) was used as the control vector. Cell transfection was performed, as described previously (16). Stable transfectants were selected for 10-14 days using G418 (Sigma, Ronkonkoma, NY) at concentration of 0.9 mg/ml in complete medium. Each plate containing hundreds of resistant clones was trypsinized and 10-20 colonies were picked up on 96-well plates, maintained in complete DMEM medium containing 0.5 mg/ml G418. After cell expansion, each clone was subject to RT-PCR assay for MT1-MMP expression and the 2 clones that stably expressed the highest level of MT1-MMP mRNA, were used for subsequent analysis. As experimental controls, a pool mixture and a single control clone were used.

*Reverse transtriptase-polymerase chain reaction (RT-PCR)*. Total RNA was extracted with Trizol reagent (Life Technologies, Gaithersburg, MD). Complementary DNA (cDNA) was generated using myeloblastosis virus reverse transcriptase (Promega, Madison, WI). Reverse transcription (RT) was performed at 42°C for 90 min, followed by heating at 95°C for 5 min (17). A housekeeping gene, phorphobilinogen deaminase (PBGD) was used as an internal control (18). The PCR primers for MT1-MMP, and PBGD are shown in Table I. PCR conditions were: initial denaturing at 95°C for 12 min, followed by 35-40 cycles of 95°C for 1 min, 62°C for 1 min and 72°C for 1 min, and a final extension at 72°C for 10 min. PCR products (661 bp) were electrophoresed on a 2% agarose gel, stained with ethidium bromide and visualized under UV transillumination.

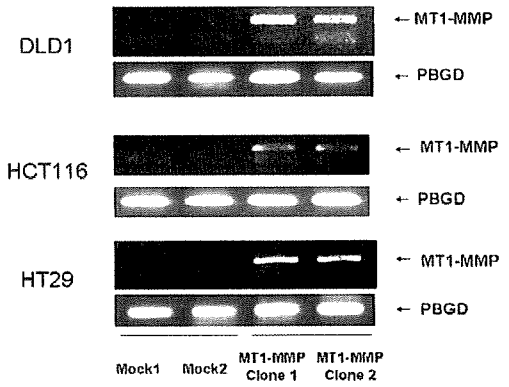


Figure 1. MT1-MMP mRNA expression. MT1-MMP mRNA expression was assessed by RT-PCR. High level of MT1-MMP mRNA was commonly noted in the stable transfectants of MT1-MMP cDNA, although endogenous MT1-MMP mRNA was scarce in three CRC cell lines. Two MT1-MMP expressing clones derived from single colony (Clone1, Clone 2) and two Mock control cultures (Mock1, pool; Mock2, single colony) are shown for each cell type. PBGD served as internal control.

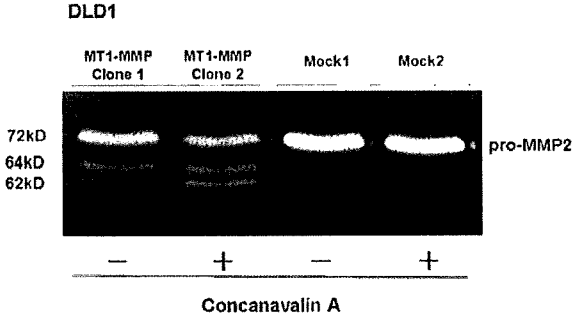


Figure 2. MT1-MMP overexpression induced gelatinolytic activity. Representative results of gelatinolytic activity in MT1-MMP expressing DLD1 cells. Both Mock controls and MT1-MMP expressing clones were treated with or without concanavalin A (Con A), which is known to enhance the cell ability to activate pro-MMP2 (19). Conditioned media were analyzed by zymography. Pro, intermediate and active forms are as indicated at 72, 64 and 62 kDa.

*Gelatin zymography*. Zymography was performed to assess the gelatinolytic activity of MT1-MMP, as previously described (19). Briefly, 24 h after seeding, cell were incubated with serum-free medium with or without 5 $\mu$M concanavalin A (Sigma) for another 48 h. Samples of conditioned medium were collected and electrophoresed on a polyacrylamide gel containing 0.1% gelatin. Substrate digestion were performed

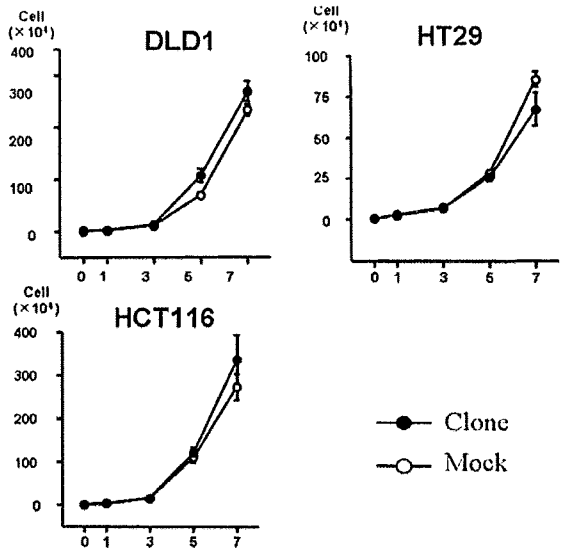


Figure 3. Cell proliferation assay. Cell counts were performed on Day 1, 3, 5 and 7. No statistically significant difference was found between the Mock control (Mock) or MT1-MMP expressing clones (Clone). Results are expressed as the mean ± SD. A repeat experiment showed similar results (data not shown).

by incubating gel in 50 mM Tris-HCl (pH 7.5) containing 5 mM $CaCl_2$, 1 $\mu$M $ZnCl_2$ at 37°C overnight with gentle rocking.

*Cell growth.* Cells were seeded at $1x10^4$ in 6-well plate in triplicate and cultured in a complete medium containing 10% FBS. Cell count was performed on day 1, 3, 5 and 7, respectively. Data were expressed as mean ± standard deviation (SD).

*Three-dimentional cell culture.* Cells were cultured in triplicate in collagen gel (Nitta Gelatin, Osaka, Japan) in 12-well plate according to manucfacturer's instructions. Collagen (1 ml) containing $5x10^5$ cells was polymerized in each well, followed by overlaying 1 ml DMEM. Culture medium was changed every 24 h. On the 10th day, the colonies >50 $\mu$m were counted in 5 fields at high magnification. Data are expressed as mean ± SD.

*Experimental liver metastasis model.* Specific pathogen-free 4-week-old BALB/c-*nu/nu* nude mice were used for *in vivo* experiments (Clea Japan, Inc., Osaka, Japan). Viable cancer cells ($5x10^6$ cell in 50 $\mu$l of cell suspension) were injected into the spleen of nude mice under light ether anesthesia, then spleen was removed after vessel ligation. Six weeks later, mice were sacrificed to determine the incidence of liver metastasis. All of the animal experiments were performed in accordance with the Guidance for the Care and Use of Laboratory Animals in Osaka University.

*Statistical analysis.* Statistical analysis was performed using the StatView J-5.0 program (Abacus Concepts, CA). Data were analyzed using Student's t-test and considered to be significant at $p<0.05$.

Table II. Incidence of liver metastasis.

| Number of foci | DLD1 | | HCT116 | | HT29 | |
|---|---|---|---|---|---|---|
| | Clone | Mock | Clone | Mock | Clone | Mock |
| 0 | 5 | 8 | 0 | 1 | 2 | 1 |
| 1-10[a] | 0 | 3 | 3 | 3 | 7 | 8 |
| Total | 5 | 11 | 3 | 4 | 9 | 9 |

[a]No mouse developed liver metastasis of >10 noduls.

## Results

*Establishment of MT1-MMP stable transfectant.* Expression of MT1-MMP mRNA in the CRC cell lines, DLD1, HCT116 and HT29 transfected with either control vector (Mock) or MT1-MMP expression plasmid (Clone), is shown in Fig. 1. Endogenous expression of MT1-MMP mRNA was scarce in 3 cell lines, while all stable tranfectants of MT1-MMP cDNA displayed an increased expression of MT1-MMP mRNA.

*Gelatinolytic activity by MT1-MMP overexpression.* The ability of MT1-MMP to activate MMP-2 was then examined using zymography. Fig. 2 showed that DLD 1 clone was able to convert pro-MMP2 (72 kD) to an active form (62 kD) and an intermediate form (64 kD). Treatment with con-canavalin A accelerated the activation process. On the other hand, the pro-MMP remained uncleaved in the Mock control cells even in the presence of concanavalin A. Similar results were obtained in two other CRC cell lines (data not shown).

*Cell proliferation assay.* In three CRC cell lines, no significant difference was noted in cell proliferation between MT1-MMP tranfectants and the Mock control cells (Fig. 3). A repeat experiment showed similar results (data not shown).

*3D cell invasion assay.* In the collagen gel, apparently invasive cell feature displaying irregular shape was observed in MT1-MMP tranfectants compared to the Mock control cells which uniformely formed small and round colonies (Fig. 4A). When the colonies with a diameter >50 $\mu$M were counted, a larger population was observed in MT1-MMP transfectants compared to the Mock control cells (Fig. 4B). Statistical significance was noted in all three cell lines.

*Effects of MT1-MMP expression on experimental liver metastasis.* We further examined the ability of liver metastatic induction between the MT1-MMP tranfectants and the Mock control cells when they were injected into the spleen. Table II showed the number of metastatic foci per mouse and the number of mouse developing liver metastasis. The size of metastatic foci was exclusively <5 mm in 3 CRC cells (data not shown). The results showed MT1-MMP expression did not affect the potential of liver metastasis. In DLD1 cells, the control cells established liver metastasis in 3 of 11 mice, but MT1-MMP transfectants did not produce hepatic metastasis

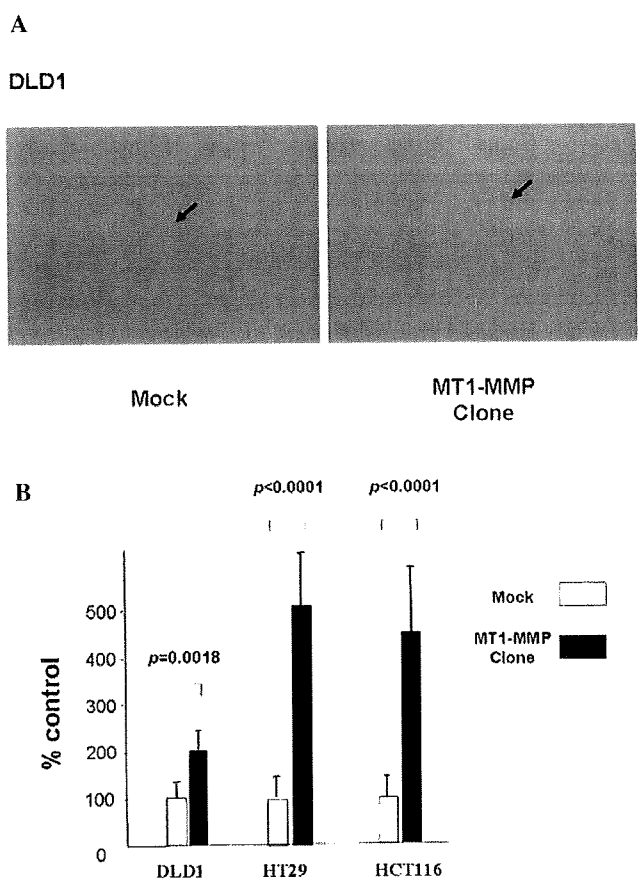


Figure 4. Cell invasion assay. (A) DLD cells cultured in collagen gel. The Mock control cells (Mock) were in tiny spherical form whereas the MT1-MMP expressing cells (Clone) were often larger and showed an expanding irregular form. These representative cells are indicated by arrows. (B) Cell count on the 10th day indicated cells >50 $\mu$m were more commonly found in MT1-MMP-expressing cells compared to Mock control cells. In each cell line, the value of Mock control was adjusted as 100%. P-value indicated statistical significance in three CRC cell lines.

at all. In HCT116 and HT29 cells, liver metastases were relatively readily established, but quite similar number and size of metastatic foci were observed between MT1-MMP clones and Mock controls.

## Discussion

MT1-MMP is implicated in the tumor invasion and metastasis process since it activates MMP-2 that degrades a major component of the basement membrane, the type IV collagen. Previous studies reported that conditional MT1-MMP over-expression contributed to enhanced potential of lymph node and lung metastasis of prostate cancer cells (20) and lymph node metastasis of gastric cancer cells (21) by orthotopic implantation model. Forced expression of MT1-MMP in tumor cells was also shown to enhance pulmonary metastases in an experimental metastasis assay (22). Liver metastasis is a frequent cause of death from CRC (13), but no study has been conducted so far to investigate whether the increased expression of MT1-MMP in CRC cells would be sufficient to induce experimental liver metastasis *in vivo*.

*In vitro* analysis of cell proliferation did not show any obvious differences between MT1-MMP overexpressing clones and the Mock control cells, indicating that expression of MT1-MMP does not stimulate proliferation of CRC cells. To date, the consensus that proteinases do not regulate tumor cell growth directly has been achieved on *in vitro* model systems wherein cancer cell behavior is classically assessed in a monolayer environment. However, it is worth noting that an increase in cell number in MT1-MMP overexpressing cells has been documented under 3D culture conditions (23,24). Putatively, when cancer cells are forced to proliferate within a dense 3D matrix, the invading capacity is a key factor that influences the tumor growth. Besides enhancement of growth of CRC cells, our results of 3D collagen cultures showed that forced expression of MT1-MMP enhanced the gelatinolytic activity, and induced invasive potential, being consistent with previous studies (25,26). These findings indicate that transduced MT1-MMP cDNA is functional in 3 CRC cell lines produced in this study.

On the contrary, increased MT1-MMP expression alone had no effect on the liver metastatic potential, when cells were injected into spleen, thus positioned directly into the blood flow. Tumor progression is a complex multistep process involving a series of different biological obstacles that a tumor cell must overcome to establish metastasis (27). Firstly, the tumor cell must invade locally, then intravasate into the circulation. Degradation of the ECM component by MMPs to remove the physical barrier is indeed the initial stage of metastasis. Soulie *et al* found that expression of MT1-MMP in non-tumorigenic, well-differentiated epithelial cells was sufficient to activate cellular responses involved in tumor initiation, local tissue invasion and intravasation (23). In the subsequent steps, at the same time, tumor cells have to execute various oncogenic properties that are required for survival in the circulation, adhesion to the endothelium, extravasation from the vessels, cell proliferation, and neovascularization. In this context, one may suppose that orthotopic implantation into the colonic wall will provide more evident effects by MT1-MMP, as reported by others (20,21). However, the scenario may not be so simple since there is evidence that forced expression of MT1-MMP in mouse carcinoma cells significantly increased number of lung nodules even in experimental metastasis assay, i.e., by injection of the cells into mouse tail vein (22). This suggests that MT1-MMP could have a role also during extravasation and/or in forming lung metastatic lesion.

It is known that the tumor-stroma interaction, especially pro-MMP2 produced by stromal cell (most probably by fibroblasts), is important for establishment of liver metastasis (3,6,12). When pro-MMP2 is activated by MT1-MMP, TIMP-2 is particular important to modulate the activity negatively (3). An imbalance between the proteolytic activity of MMP-2 and TIMP-2 is shown to be clinically important in hepatocellar carcinoma, gall bladder carcinoma, and hilar cholangiocarcinoma (28-30). Moreover, Brand *et al* previously reported that adenoviral transfer of TIMP-2 into the liver tissue suppressed liver metastasis (31). Therefore, another possibility might be that the conditional MT1-MMP overexpression *in vivo* could be counteracted by TIMP-2 derived from liver tissue.

Undoubtedly, MT1-MMP has a role in tumor invasion and metastasis. However, our data showed that MT1-MMP expression led to the development of invasive properties of CRC cells but these characteristics were insufficient to promote the formation of liver metastasis in mouse experimental model. Our findings suggest that a more complicated mechanism may be involved in the activation and regulation of MMPs cascades *in vivo* metastasis to liver.

**Acknowledgements**

We are grateful to Nobuaki Hiraoka for valuable technical advice in gelatinolytic activity assay and invasion assay in collagen.

**References**

1. Hornebeck W, Emonard H, Monboisse JC and Bellon G: Matrix-directed regulation of pericellular proteolysis and tumor progression. Semin Cancer Biol 12: 231-241, 2002.
2. Nagase H: Activation mechanisms of matrix metalloproteinases. Biol Chem 378: 151-160, 1997.
3. Osenkowski P, Toth M and Fridman R: Processing, shedding, and ecdocytosis of membrane type 1-matrix metalloproteinase (MT1-MMP). J Cell Physiol 200: 2-10, 2004.
4. Curran S and Murray GI: Matrix metalloproteinases: molecular aspects of their roles in tumour invasion and metastasis. Eur J Cancer 36: 1621-1630, 2000.
5. Sato H, Takino T, Okada Y, Cao J, Shinagawa A, Yamamoto E and Seiki M: A matrix metalloproteinase expressed on the surface of invasive tumour cells. Nature 370: 61-65, 1994.
6. Maquoi E, Frankenne F, Baramova E, *et al*: Membrane type 1 matrix metalloproteinase-associated degradation of tissue inhibitor of metalloproteinase 2 in human tumor cell lines. J Biol Chem 275: 11368-11378, 2000.
7. Uekita T, Itoh Y, Yana I, Ohno H and Seiki M: Cytoplasmic tail-dependent internalization of membrane-type 1 matrix metalloproteinase is important for its invasion-promoting activity. J Cell Biol 155: 1345-1356, 2001.
8. Kikuchi R, Noguchi T, Takeno S, Kubo N and Uchida Y: Immunohistochemical detection of membrane-type-1-matrix metalloproteinase in colorectal carcinoma. Br J Cancer 83: 215-218, 2000.
9. Deryugina EI, Soroceanu L and Strongin AY: Up-regulation of vascular endothelial growth factor by membrane type 1 matrix metalloproteinase stimulates human glioma xenograft growth and angiogenesis. Cancer Res 62: 580-588, 2002.
10. Seiki M: Membrane-type 1 matrix metalloproteinase: a key enzyme for tumor invasion. Cancer Lett 194: 1-11, 2003.
11. Malhotra S, Newman E, Eisenberg D, Scholes J, Wieczorek R, Mignatti P and Shamamian P: Increased membrane type a matrix metalloproteinase expression from adenoma to colon cancer: a possible mechanism of neoplastic progression. Dis Colon Rectum 45: 537-543, 2002.
12. Curran S, Dundas SR, Buxton J, Leeman MF, Ramsay R and Murray GI: Matrix metalloproteinase/tissue inhibitors of matrix metalloproteinase phenotype identifies poor prognosis colorectal cancers. Clin Cancer Res 10: 8229-8234, 2004.
13. Kobayashi H, Mochizuki H, Sugihara K, *et al*: Characteristics of recurrence and surveillance tools after curative resection for colorectal cancer: a multicenter study. Surgery 141: 67-75, 2007.
14. Pei D and Weiss SJ: Transmembrane-deletion mutants of the membrane-type matrix metalloproteinase-1 process progelatinase A and express intrinsic matrix-degrading activity. J Biol Chem 271: 9135-9140, 1996.
15. Yana I and Weiss S: Regulation of membrane type-1 matrix metalloproteinase activation by proprotein convertases. Mol Biol Cell 11: 2387-2401, 2000.
16. Deryugina EI, Bourdon MA, Luo GX, Reisfeld RA and Strongin A: Matrix metalloproteinase-2 activation modulates glioma cell migration. J Cell Sci 110: 2473-2482, 1997.
17. Ogawa M, Yamamoto H, Nagano H, *et al*: Hepatic expression of ANG2 RNA in metastatic colorectal cancer. Hepatology 39: 528-539, 2004.
18. Chretien S, Dubart A, Beaupain D, *et al*: Alternative transcription and splicing of the human porphobilinogen deaminase gene result either in tissue-specific or in housekeeping expression. Proc Natl Acad Sci USA 85: 6-10, 1988.
19. Okami J, Nakamori S, Hiraoka N, *et al*: Suppression of pancreatic cancer cell invasion by a cyclooxygenase-2-specific inhibitor. Clin Exp Metastasis 20: 577-584, 2003.
20. Cao J, Chiarelli C, Kozarekar P and Adler HL: Membrane type1-matrix metalloproteinase promotes human prostate cancer invasion. Thromb Haemost 93: 770-778, 2005.
21. Yonemura Y, Endo Y, Takino T, *et al*: Membrane-type 1 matrix metalloproteinase enhances lymph nodes metastasis of gastric cancer. Clin Exp Metastasis 18: 321-327, 2000.
22. Tsunezuka Y, Kinoh H, Takino T, *et al*: Expression of membrane-type matrix metalloproteinase (MT1-MMP) in tumor cells enhances pulmonary metastases in an experimental metastasis assay. Cancer Res 56: 5678-5683, 1996.
23. Soulie P, Carrozzino F, Pepper MS, Strongin AY, Poupon MF and Montesano R: Membrane-type-1 matrix metalloproteinase confers tumorigenicity on nonmalignant epithelial cells. Oncogene 24: 1689-1697, 2005.
24. Hotary KB, Allen ED, Brooks PC, Datta NS, Long MW and Weiss SJ: Membrane type I matrix metalloproteinase usurps tumor growth control imposed by the three-dimensional extracellular matrix. Cell 114: 33-45, 2003.
25. Wang P, Nie J and Pei D: The hemopexin domain of membrane-type matrix metalloproteinase-1 (MT1-MMP) is not required for its activation of proMMP2 on cell surface but is essential for MT1-MMP-mediated invasion in three-dimensional type I collagen. J Biol Chem 279: 51148-51155, 2004.
26. Bartolome RA, Galvez BG, Longo N, *et al*: Stromal cell-derived factor-1alpha promotes melanoma cell invasion across basement membranes involving stimulation of membrane-type 1 matrix metalloproteinase and Rho GTPase activities. Cancer Res 64: 2534-2543, 2004.
27. Kohn EC and Liotta LA: Invasion and metastasis: new approaches to an old problem. Oncology 7: 47-52, 1993.
28. Giannelli G, Bergamini C, Marinosci F, *et al*: Clinical role of MMP-2/TIMP-2 imbalance in hepatocellular carcinoma. Int J Cancer 97: 425-431, 2002.
29. Fan YZ, Zhang JT, Yang HC and Yang YQ: Expression of MMP-2,TIMP-2 protein and the ratio of MMP-2/TIMP-2 in gall-bladder carcinoma and their significance.World J Gastroenterol 8: 1138-1143, 2002.
30. Xiao M, Zhou NX, Huang ZQ, Lu YL, Chen LH, Wang DJ and Chang WL: The ratio of MMP-2 to TIMP-2 in hilar cholangio-carcinoma: a semi-quantitative study. Hepatobiliary Pancreat Dis Int 3: 599-602, 2004.
31. Brand K, Baker AH, Perez-Cantó A, Possling A, Sacharjat M, Geheeb M and Arnold W: Treatment of colorectal liver metastases by adenoviral transfer of tissue inhibitor of metallo-proteinases-2 into the liver tissue. Cancer Res 60: 5723-30, 2000.